Vector-relation configurations and plabic graphs

Niklas Affolter, Max Glick, Pavlo Pylyavskyy, Sanjay Ramassamy

VECTOR-RELATION CONFIGURATIONS AND PLABIC GRAPHS

NIKLAS AFFOLTER, MAX GLICK, PAVLO PYLYAVSKYY, AND SANJAY RAMASSAMY

Abstract. We study a simple geometric model for local transformations of bipartite graphs. The state consists of a choice of a vector at each white vertex made in such a way that the vectors neighboring each black vertex satisfy a linear relation. Evolution for different choices of the graph coincides with many notable dynamical systems including the pentagram map, Q-nets, and discrete Darboux maps. On the other hand, for plabic graphs we prove unique extendability of a configuration from the boundary to the interior, an elegant illustration of the fact that Postnikov's boundary measurement map is invertible. In all cases there is a cluster algebra operating in the background, resolving the open question for Q-nets of whether such a structure exists.

1. Introduction

The dynamics of local transformations on weighted networks plays a central role in a number of settings within algebra, combinatorics, and mathematical physics. In the context of the dimer model on a torus, these local moves give rise to the discrete cluster integrable systems of Goncharov and Kenyon [13]. Meanwhile, for plabic graphs in a disk, Postnikov transformations relate different parametrizations of positroid cells [26] which in turn define a stratification of the totally non-negative Grassmannian.

The dimer model also manifests itself in many geometrically defined dynamical systems. We focus on projective geometry and draw our initial motivation from the pentagram map. The pentagram map was defined by Schwartz [28] and related to coefficient-type cluster algebra dynamics in [11]. Gekhtman, Shapiro, Tabachnikov, and Vainshtein [9, 10] placed the pentagram map and certain generalizations in the context of weighted networks and derived a more conceptual take on the integrability property first proven by Ovsienko, Schwartz, and Tabachnikov [24]. Although considerable work in various directions of the subject has been undertaken, most relevant to our work is a further generalization termed Y-meshes [12].

We propose a simple but versatile geometric model for the space of edge weights of any bipartite graph modulo gauge equivalence. The induced dynamics of local transformations includes in special cases pentagram maps, Q-nets, and discrete Darboux maps. This common generalization resolves a long standing question of how the pentagram map and Q-nets relate. Moreover, our systems come with a cluster dynamics, which is new in the Q-net case. Lastly, in the setting of plabic graphs we define a geometric version of the boundary measurement map and its inverse. In this language, properties of the boundary measurement map imply unique solvability of a certain family of geometric realization problems.

Let G be a planar bipartite graph with vertex set $B \cup W$. For $b \in B$ let $N(b) \subseteq W$ denotes its set of neighbors. Fix a vector space V.

Definition 1.1. A *vector-relation configuration* on G consists of choices of

- a nonzero vector $v_w \in V$ for each $w \in W$ and
- a non-trivial linear relation R_b among the vectors $\{v_w : w \in N(b)\}$ for each $b \in B$.

In particular, each set $\{v_w : w \in N(b)\}$ must be linearly dependent.

By a linear relation we mean a formal linear combination of vectors that evaluates to zero. For technical reasons it is best to allow G to have multiple edges in which case the $N(B)$ are understood to be multisets and a given vector can appear multiple times in a given relation. We often ignore this possibility, either implicitly or by assuming G to be reduced (a certain condition that implies it lacks multiple edges).

Definition 1.2. Consider a vector-relation configuration on a graph G as above and suppose $\lambda \neq 0$. The *gauge transformation* by λ at a black vertex $b \in B$ scales the relation R_b by λ (and keeps all other vectors and relations the same). The *gauge transformation* by λ at a white vertex $w \in W$ scales v_w by $1/\lambda$ and scales the coefficient of v_w by λ in each relation in which it appears to compensate. Two vector-relation configurations are called *gauge equivalent* if they are related by a sequence of gauge transformations.

Gauge equivalence classes of vector-relation configurations serve as our main object of study. For the remainder of the introduction, we define both local transformations and a boundary measurement type map for such configurations, and present our main results.

Key words and phrases. Pentagram map, plabic graphs, dimer model.

N. A. was supported by DFG SFB/Transregio 109 "Discretization in Geometry and Dynamics". P. P. was partially supported by NSF grants DMS-1148634 and DMS-1351590. S.R. was partially supported by the ANR-18-CE40-0033 project DIMERS..

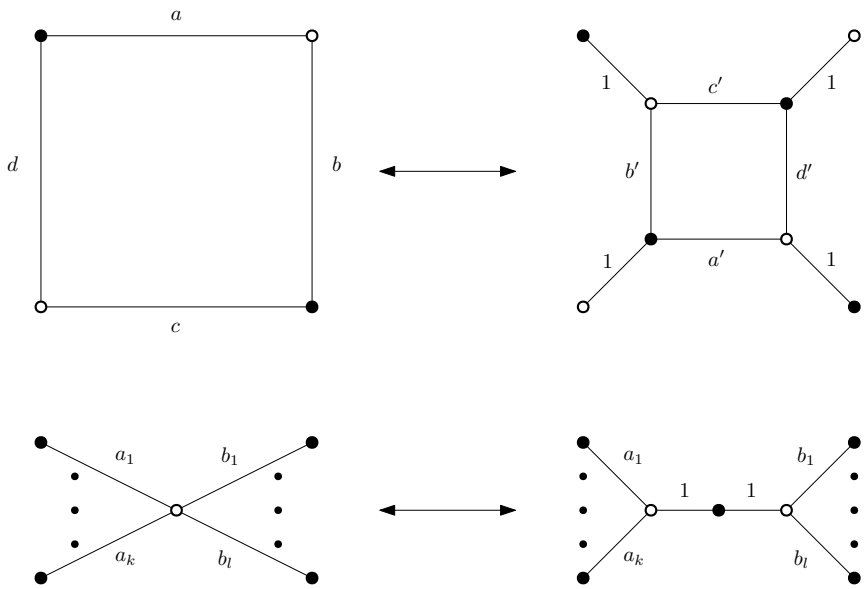

FIGURE 1. Local transformations applied to a graph.

1.1. **Local transformations.** Let G be a planar bipartite graph with nonzero edge weights. A *gauge transformation* at a given vertex multiplies the weights of all edges incident to that vertex by a common scalar. A *local transformation* modifies a small portion of G in the manner indicated in one of the pictures in Figure 1. There are two types of local transformations:

- The top of Figure 1 depicts *urban renewal*. The new edge weights are

$$a' = \frac{a}{ac+bd}, \quad b' = \frac{b}{ac+bd}, \quad c' = \frac{c}{ac+bd}, \quad d' = \frac{d}{ac+bd}. \tag{1.1}$$

- The bottom of Figure 1 depicts *degree two vertex addition*. A vertex is split into two vertices of the same color connected by a new degree two vertex of the opposite color. The move depends on a choice of a partition of the neighbors of the original vertex into two cyclically consecutive blocks of size k and l. The figure depicts addition of a degree two black vertex, but the same move is allowed with all colors reversed producing a degree two white vertex instead.

It is common to consider the space of edge-weightings of G modulo gauge equivalence, and it is easy to see that local transformations are well-defined on this level. Both types of local moves can be performed in either direction, where going from right to left requires first applying gauges to make the indicated edge weights equal to 1. The second local transformation when applied from right to left is called *degree two vertex removal*.

We now wish to define dynamics with the same combinatorics as local transformations, but operating on our vector and relation data rather than on edge weights. If R is a relation among vectors $\{u_1, \dots, u_k, v_1, \dots, v_l\}$ let $R|_{u_1 \cdots u_k}$ denote the linear combination of $u_1, \dots, u_k$ appearing in R. This combination may be formal or not depending on context. For instance, as formal linear combinations we have $R|_{u_1 \cdots u_k} + R|_{v_1 \cdots v_l} = R$ while as vectors we have $R|_{u_1 \cdots u_k} + R|_{v_1 \cdots v_l} = 0$ since R evaluates to 0.

First consider urban renewal, as pictured in Figure 2. We need to define the vectors and relations at the new vertices. Let $u_1 = R_1|_{v_1 v_2}$ and $u_2 = R_2|_{v_1 v_2}$. Note u_1 and u_2 are both given as linear combinations of v_1, v_2, so if the coefficient matrix is nonsingular we can formally solve for each v_i in terms of u_1 and u_2. Moving the u_j terms to the other side we get a linear relation S_i among v_i, u_1, and u_2 for $i = 1, 2$. In short, the u_i, v_i and S_i are consistent with being part of a vector-relation configuration on the new graph. As a final step R_1 is modified to reflect that a linear combination of v_1, v_2 has been replaced by $1u_1$ and similarly with R_2.

Next consider degree two vertex addition, as picture in Figure 3. First suppose we are adding a degree two black vertex. It is natural to set the new vectors equal to each other and to the old vector, i.e. $v = w = u$. We then get a relation $T = 1v - 1w$. The nearby relations do not need to be modified at all. On the other hand, suppose we are adding a degree two white vertex. Choose as the new vector $w = R|_{u_1 \cdots u_k} = -R|_{v_1 \cdots v_l}$. We get the relation S by starting with R and replacing $R|_{v_1 \cdots v_l}$ with $-1w$. Similarly T is obtained from R by replacing $R|_{u_1 \cdots u_k}$ with $1w$.

As with classical local transformations, these operations preserve gauge equivalence and can be run in both directions. In fact, we will show (Proposition 2.1) that these two stories are in some sense equivalent to each other. At least locally, it is possible to go back and forth between edge weights and vector-relation configurations (with some genericity assumptions) in a manner that commutes with local transformations. As a result, we

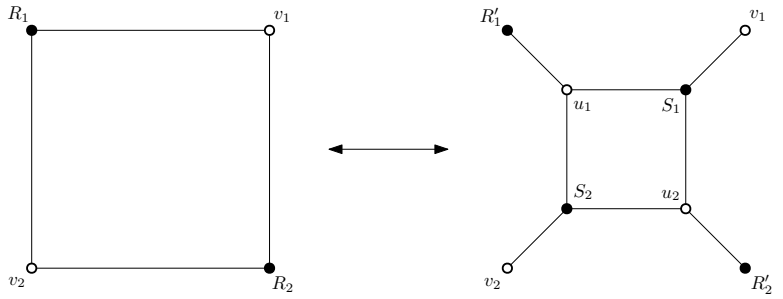

FIGURE 2. The vector-relation version of urban renewal.

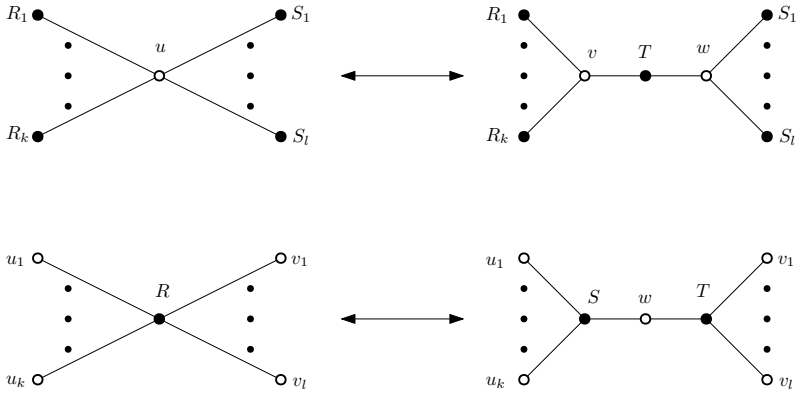

FIGURE 3. The vector-relation version of degree two vertex addition.

can import much of the theory of the dimer model to our setting. For instance we get face weights, which are simple to define geometrically and which satisfy nice evolution equations.

1.2. **Configurations on plabic graphs.** Plabic graphs are a family of finite planar graphs widely used in the study of positroids and the totally non-negative Grassmannian. Restricted to this case, our model provides a new take on plabic graphs and much of the surrounding theory.

A *plabic graph* is a finite planar graph $G = (B \cup W, E)$ embedded in a disk with the vertices all colored black or white. We assume throughout that G is in fact bipartite, that all of its boundary vertices are colored white, and that each boundary vertex has degree 1 or 0. An *almost perfect matching* of G is a matching that uses all internal vertices (and some boundary vertices). Assume always that G has at least one almost perfect matching.

Remark 1.3. The most common formulation these days [21, 23] is to assume that G is bipartite with the boundary vertices being uncolored and all having degree 1. Starting from such a graph, one can use degree 2 vertex addition where needed on boundary edges to get each boundary vertex adjacent to a black vertex. At that point, boundary vertices can be colored white to adhere to our conventions. The exception is if the original graph has a degree 1 white vertex attached to the boundary. The above procedure would produce a graph that is not reduced, a condition we will eventually require. For us, an isolated boundary vertex models this situation.

Fix for the moment a plabic graph $G = (B \cup W, E)$. Let $M = |B|$, $N = |W|$, and let n be the number of boundary vertices. As all boundary vertices are white that leaves $N - n$ internal white vertices. Number the elements of B and W respectively 1 through M and 1 through N in such a way that the boundary (white) vertices are numbered 1 through n in clockwise order. We will sometimes use these numbers in place of the vertices, e.g. writing v_i for the vector of a configuration at the white vertex numbered i. Let $k = N - M$. Each almost perfect matching uses all M black vertices and all $N - n$ internal white vertices. As such it must use $M - (N - n) = n - k$ boundary vertices, from which we conclude $0 \leq k \leq n$, with the interesting case being $0 < k < n$.

We make several modifications to our model to better cater to plabic graphs and related geometry. First, we will see the natural ambient dimension is $k = N - M$ so we simply fix as our vector space $V = \mathbb{C}^k$. It is also natural to allow boundary vectors to be zero, and to add some genericity assumptions. In the following, let K_{ij} denote the coefficient of the vector v_j in relation R_i where $1 \leq i \leq M$ and $1 \leq j \leq N$.

Definition 1.4. A *vector-relation configuration* on a plabic graph G is a choice of vector $v_w \in V = \mathbb{C}^k$ for each $w \in W$ and a non-trivial linear relation R_b among the neighboring vectors of each $b \in B$ such that

- the vector v_w at each internal white vertex w is nonzero,
- the boundary vectors $v_1, \dots, v_n$ span V, and
- the $M \times N$ matrix $K = (K_{ij})$ is full rank.

Two configurations are called *gauge equivalent* if they are related by a sequence of gauge transformations, in the sense of Definition 1.2, at internal vertices.

Although local transformations are also of interest in this case, we focus on global questions concerning the space of all configurations given fixed G. The main result, which in isolation is rather striking, is that a configuration is uniquely determined up to gauge by its boundary vectors.

To state this result precisely, and also to provide relevant context, we need notions from positroid theory. Recall that for G as above every almost perfect matching of G uses $n-k$ of the n boundary vertices. The *positroid* $\mathcal{M} = \mathcal{M}(G)$ associated to G is the set of k element subsets $J \subseteq \{1, \dots, n\}$ such that G has an almost perfect matching using the boundary vertices not in J.

The significance of positroids lies in their use in the study, initiated by Postnikov [26], of the totally nonnegative Grassmannian. Let $A \in Gr(k,n)$ viewed as a $k \times n$ matrix and let $\Delta_J(A)$ denote the Plücker coordinate of A given by the maximal minor of A using column set J. Positroids $\mathcal{M}$ as constructed above are characterized by the property that there exists A such that $\Delta_J(A) \geq 0$ for all J, i.e. A is *totally nonnegative*, and $\Delta_J(A) > 0$ precisely for $J \in \mathcal{M}$. The set of such A is a topological cell and can be parametrized by a function on edge weights of G called the boundary measurement map.

As mentioned previously, there is a correspondence between edge weightings of a graph and certain vector-relation configurations thereon. We will show (Proposition 4.9) that the boundary measurement map translates simply to restriction of a configuration to the boundary. More precisely, the point of the Grassmannian associated to a vector-relation configuration $(\mathbf{v}, \mathbf{R})$ is $A = [v_1 \cdots v_n]$ (recall $V = \mathbb{C}^k$ so each boundary vector v_i has k entries). We allow complex, and in some cases zero, edge weights. As such the space of potential outputs is the full *positroid variety* $\Pi_{\mathcal{M}}$ defined in the Grassmannian by the equations $\Delta_J = 0$ for all $J \notin \mathcal{M}$.

Theorem 1.5. *Fix a plabic graph G with all the preceding conventions and notation.*

(1) If $(\mathbf{v}, \mathbf{R})$ is a vector-relation configuration on G then $A = [v_1 \cdots v_n]$ lies in the Positroid variety $\Pi_{\mathcal{M}}$.
(2) Suppose G is reduced. For generic $A \in \Pi_{\mathcal{M}}$, the columns $v_1, \dots, v_n$ of A can be extended to a vector-relation configuration on G that is unique up to gauge at internal vertices. In particular, each internal vector is determined up to scale.

We delay the definition of reducedness for plabic graphs to Section 4.1, which also contains background on various aspects of positroid theory. Also, note that in examples such as the following we allow boundary vertices to have degree greater than 1. Our main results can be generalized to this situation, but it makes some definitions and arguments more cumbersome.

Example 1.6. Consider the plabic graph G in Figure 4. It has $k = 3$ and $n = 6$. In fact, the associated positroid is the uniform matroid, meaning all 3 element subsets of $\{1, \dots, 6\}$ are included. So the positroid variety is the whole Grassmannian $Gr_{3,6}$. In short, the boundary vectors $v_1, \dots v_6 \in \mathbb{C}^3$ of a configuration can be generic.

Now suppose $v_1, \dots v_6 \in \mathbb{C}^3$ are given and consider the possibilities for the internal vector u. The lower black vertex forces u, v_1, v_2 to be dependent while the top black vertex forces u, v_4, v_5 to be dependent. If the v_i are generic then u must lie on the line of intersection of the planes $\langle v_1, v_2 \rangle$ and $\langle v_4, v_5 \rangle$. Hence u is determined up to scale. The other two black vertices have degree 4. It is always possible to find a linear relation among 4 vectors in $\mathbb{C}^3$, so there are no added conditions imposed on u.

1.3. **Relation to previous work.** Our model of vector-relation configurations has substantial precedent in the literature. In fact, a main selling point of our specific formulation is that it is versatile enough to tie into previously studied ideas in a variety of areas. We outline some of the relevant previous work here for the interested reader's convenience.

In the plabic graph setting, Lam's *relation space* [21, Section 14] is in a sense dual to our model. Let G be a plabic graph and suppose we have vectors $v_w \in \mathbb{C}^k$ at white vertices satisfying relations

$$\sum_w K_{bw} v_w = 0$$

indexed by black vertices. Our approach is to consider the boundary vectors $[v_1 \cdots v_n]$ as making up a point in $Gr_{k,n}$. The relation space is the dual point of $Gr_{n-k,n}$. More directly, one takes in the n-dimensional space of linear combinations of $v_1, \dots, v_n$ the subspace consisting of valid relations. Note that the coefficients K_{bw} alone determine the relation space, so the v_w are replaced with formal variables. In light of this connection, our Proposition 4.9 is equivalent to [21, Theorem 14.6] except that we give explicit rules for the signs.

Another geometric model on plabic graphs is provided by Postnikov [25]. He associates a point of a small Grassmannian $Gr_{1,3}$ or $Gr_{2,3}$ to each vertex. His setup has the advantage that there is a natural duality

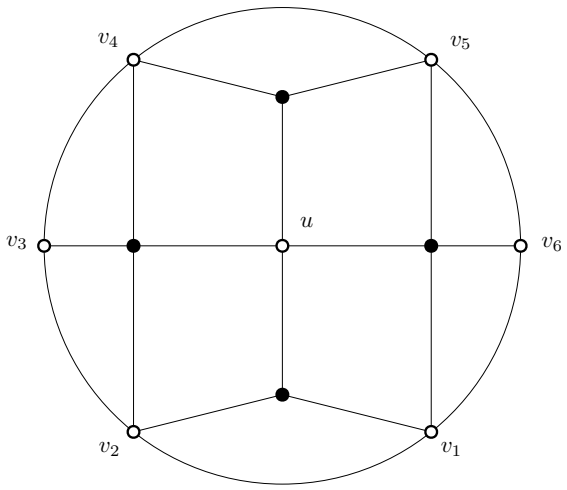

FIGURE 4. A plabic graph corresponding to the open cell in $Gr(3,6)$

between the black and white vertices. We should also note that both [21, Section 14] and [25] are attempts to put on more mathematical footing the on-shell diagrams of physics.

In the case of the dimer model on the torus, Kenyon and Okounkov [16] associate a section of a certain line bundle to each white vertex of a bipartite graph. It is easy to see that said sections satisfy linear relations in such a way as to give a configuration (in an infinite dimensional space). Fock [7] shows how to recover this data from the line bundle. He constructs on each vertex of one color (black with his conventions) a one dimensional space defined by a certain intersection of spaces living on zigzags. Our reconstruction map for plabic graphs as defined by (4.8) is entirely analogous.

As already mentioned, Gekhtman et al. [9, 10] were the first to describe the pentagram map (and generalizations) in terms of dynamics on networks. It is easy in retrospect to see all of the ideas of vector-relation configurations in these papers. For instance, the authors identify the edge weights as coefficients of linear relations among lifts of the points of the polygon. Such coefficients also appear as the a, b-coordinates of Ovsienko, Schwartz, and Tabachnikov [24]. Similarly, in the study of Q-nets [3] an important role is played by the relation among the four coplanar points living at the vertices of each primitive square.

Finally, we note that there are many other geometric models on planar bipartite graphs compatible with the dimer model on the torus, for instance T-graphs [18], Miquel dynamics on circle patterns [1, 15], and Clifford dynamics [20]. The interplay between the various models is considered in [2]. That paper also includes descriptions of both Q-nets and discrete Darboux maps in terms of cluster dynamics arrived at independently from those in the present paper.

1.4. **Structure of the paper.** The remainder of this paper is organized as follows. Section 2 covers the basic properties of our vector-relation model as well as a slight modification living in projective space. In Section 3 we illustrate how to incorporate several previously studied systems into our framework. We tackle the plabic graph case in Sections 4 and 5. More specifically, Section 4 builds the general theory and proves Theorem 1.5, while Section 5 considers the geometry of the space of configurations on a plabic graph. Lastly, in Section 6 we identify what sorts of vector-relation configurations arise from resistor and Ising networks.

Acknowledgments. We thank Lie Fu, Rick Kenyon, and Kelli Talaska for many helpful conversations.

2. Vector-relation configurations

In this section we develop the theory of vector-relation configurations on general planar bipartite graphs as in Definitions 1.1 and 1.2. To that end, let $G = (B \cup W, E)$ be a planar bipartite graph. We will denote a vector-relation configuration on G by $(\mathbf{v}, \mathbf{R})$ (or sometimes just $\mathbf{v}$ for short) where $\mathbf{v} = (v_w)_{w \in W}$ and $\mathbf{R} = (R_b)_{b \in B}$.

2.1. **Constructing the edge weights.** For $b \in B$ and $w \in W$, let K_{bw} denote the coefficient of v_w in R_b, understood to be 0 if b, w are not adjacent in G. Performing local moves sometimes requires $K_{bw} \neq 0$ for certain $\overline{bw} \in E$, so we add that assumption when needed. If G is finite then we can view K as a $|B|$-by-$|W|$ matrix. Gauge transformations correspond to multiplying rows and/or columns of K by nonzero scalars.

The matrix K plays the part of the Kasteleyn matrix in the dimer model. As such, certain signs are required to obtain the edge weights. Specifically, suppose a choice of $\varepsilon_{bw} = \pm 1$ on each edge $\overline{bw} \in E$ is made so that

- each $4k$-gon face of G has an odd number of -1's on its boundary, while
- each $(4k+2)$-gon face of G has an even number of -1's on its boundary.

Let $\mathrm{wt}(e) = \varepsilon_{bw} K_{bw}$ for each edge $e = \overline{bw}$ of G. Assuming the edge weights are nonzero, we obtain what is called a trivialized line bundle with connection [13] on G. Note in the planar case that any two choice of Kasteleyn signs are gauge equivalent, so the gauge class of the result depends only on the gauge class of $(\mathbf{v}, \mathbf{R})$.

Proposition 2.1. *Let $(\mathbf{v}, \mathbf{R})$ be a vector-relation configuration on G. Apply a local transformation to obtain a new configuration $(\mathbf{v}', \mathbf{R}')$ on G'. Then the weight functions associated to these two configurations are related by a classical local transformation.*

Proof. First suppose the operation is urban renewal, and adopt the notation of Figure 2. Suppose the initial relations are

$$R_1 = \widetilde{a} v_1 + \widetilde{d} v_2 + \dots$$
$$R_2 = \widetilde{b} v_1 + \widetilde{c} v_2 + \dots$$

so by definition $u_1 = \widetilde{a} v_1 + \widetilde{d} v_2$ and $u_2 = \widetilde{b} v_1 + \widetilde{c} v_2$. Therefore

$$v_1 = \frac{\widetilde{c} u_1 - \widetilde{d} u_2}{\widetilde{a}\widetilde{c} - \widetilde{b}\widetilde{d}}$$
$$v_2 = \frac{-\widetilde{b} u_1 + \widetilde{a} u_2}{\widetilde{a}\widetilde{c} - \widetilde{b}\widetilde{d}}$$

The new relations are

$$S_1 = v_1 + \widetilde{c}' u_1 + \widetilde{d}' u_2$$
$$S_2 = v_2 + \widetilde{b}' u_1 + \widetilde{a}' u_2$$

where

$$\widetilde{a}' = \frac{-\widetilde{a}}{\widetilde{a}\widetilde{c} - \widetilde{b}\widetilde{d}}, \quad \widetilde{b}' = \frac{\widetilde{b}}{\widetilde{a}\widetilde{c} - \widetilde{b}\widetilde{d}}, \quad \widetilde{c}' = \frac{-\widetilde{c}}{\widetilde{a}\widetilde{c} - \widetilde{b}\widetilde{d}}, \quad \widetilde{d}' = \frac{\widetilde{d}}{\widetilde{a}\widetilde{c} - \widetilde{b}\widetilde{d}}. \tag{2.1}$$

Let $a, b, c, d, a', b', c', d'$ be the edge weights obtained by multiplying the associated coefficients by Kasteleyn signs. The notation has been chosen so that these weights correspond to edges in the manner indicated in Figure 1. On the left is a quadrilateral face which should have an odd number of -1's. Applying gauge we can assume specifically $a = -\widetilde{a}$, $b = -\widetilde{b}$, $c = -\widetilde{c}$, and $d = \widetilde{d}$. It is consistent on the right to have the edge labeled b' be negative, all other pictured edges positive, and all edges outside the picture keeping their original signs. So we put $a' = \widetilde{a}'$, $b' = -\widetilde{b}'$, $c' = \widetilde{c}'$, and $d' = \widetilde{d}'$. Applying this substitution to (2.1) verifies that the edge weights evolve according to (1.1), as desired.

Now suppose the transformation is degree 2 vertex addition. There is a natural injection from edges of G to edges of G', and the definitions are such that coefficients living on these edges are all unchanged. Fixing Kasteleyn signs on G, we can get valid signs on G' by keeping the signs of all old edges and giving the two new edges opposite signs from each other. If the new vertex is black (see top of Figure 3), the opposite signs are reflected in the new relation $T = 1v - 1w$. If instead it is white (bottom of Figure 3) we have that the new vector w appears with coefficient -1 in S and $+1$ in T, so again the signs are opposite. In both cases, the unsigned weights of both new edges equal 1 in agreement with the bottom of Figure 1. □

Note that the map from vector-relation configurations to line bundles with connection on G has only been defined in the one direction. Before moving on to applications, we briefly discuss the reverse problem. Suppose a planar bipartite graph $G = (B \cup W, E)$ is given with edge weights. Applying Kasteleyn signs we obtain formal relations. One approach to getting the vectors is to start with $|W|$ independent vectors and quotient the ambient space by these relations. The resulting configuration is the most general with these edge weights in the sense that any other will be a projection of it. In particular, assuming highest possible dimension the configuration is unique up to linear isomorphism. We explore this construction in the Plabic graph case in Section 4.

A more difficult matter is existence of a configuration for given edge weights. A fundamental family of examples come from taking G to be balanced (same number of white and black vertices) on a torus. In this case, the construction from the previous paragraph applied to generic edge weights would produce a trivial configuration with all vectors equals to 0. A partial remedy would be to allow twisted configurations in the spirit of twisted polygons in the theory of the pentagram map.

2.2. **The face weights.** For a line bundle with connection on G, the basic gauge invariant functions are the *monodromies* around closed cycles. In terms of edge weights, the monodromy is the product of weights along the cycle taken alternately to the power 1 and -1. We can pull these quantities back to get gauge invariant functions of vector-relation configurations.

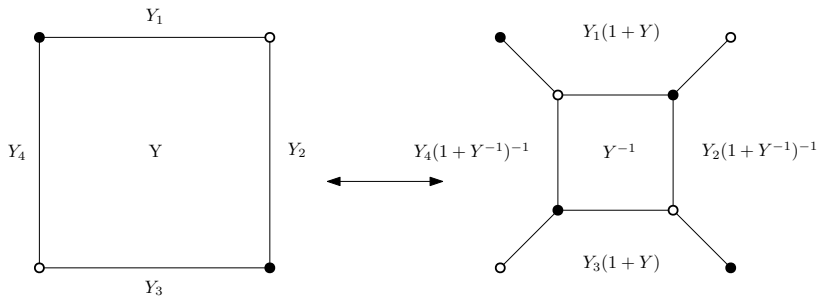

FIGURE 5. The evolution equation for face weights

We focus on the case of the monodromy around a single face F of G. Suppose F is a $2m$-gon and that the vertices on its boundary in clockwise order are $w_1, b_1, \ldots, w_m, b_m$. The *face weight* of a vector-relation configuration corresponding to F is

$$Y_F = (-1)^{m-1} \frac{K_{b_1 w_1} K_{b_2 w_2} \cdots K_{b_m w_m}}{K_{b_1 w_2} K_{b_2 w_3} \cdots K_{b_m w_1}}. \tag{2.2}$$

The sign accounts for the product of Kasteleyn signs around the face.

Proposition 2.2. *Under an urban renewal move, the face weights of a vector-relation configuration evolve as in Figure 5. The face weights are unchanged by degree* 2 *vertex addition/removal.*

Proof. The formulas follow from the case of ordinary local transformations, for which they are standard, see e.g. [13, Theorem 4.7]. □

To simplify some formulas, we introduce a vector associated to each black vertex b of a given face F. Suppose w and w' are the neighbors of b around F. Given a vector relation configuration we define $v(F,b) = R_b|_{ww'} = K_{bw} v_w + K_{bw'} v_{w'}$. The v_w and $v(F,b)$ for w and b around F contain the data needed to calculate Y_F. Moreover, if F is a quadrilateral and b, b' its black vertices, then the two new vectors arising from urban renewal at F are $v(F,b)$ and $v(F,b')$.

2.3. **Projective dynamics.** By placing an additional assumption on our configurations, we can obtain an elegant model for the gauge classes in terms of projective geometry. Recall a set of vectors is called a *circuit* if it is linearly dependent but each of its proper subsets is linearly independent. Say that a vector-relation configuration is a *circuit configuration* if each set $\{v_w : w \in N(b)\}$ is a circuit for $b \in B$. For each $w \in W$, let P_w equal the span of v_w considered as a point in the projective space $\mathbb{P}(V)$.

Proposition 2.3. *The gauge class of a circuit configuration is uniquely determined by the configurations of points $P_w \in \mathbb{P}(V)$ for $w \in W$.*

Proof. Suppose two circuit configurations both give rise to the points P_w. Then the vectors agree up to scale, so we can gauge to get the vectors v_w to agree exactly. It remains to show that for each $b \in B$ the relations R_b and R'_b on $\{v_w : w \in N(b)\}$ of the two configurations agree up to scale. If not one could find a linear combination of R_b and R'_b with a zero coefficient, violating the circuit condition around b. □

As usual, we take an affine chart to visualize $\mathbb{P}(V)$ as an affine space of dimension one less than V. From this point of view, a circuit of size d consists of d points contained in an $d-2$ dimensional plane with each proper subset in general position (e.g. 4 points on a plane of which no 3 are collinear).

We next describe how local transformations look on the level of the P_w. For F a face of G and w_1, b, w_2 three consecutive vertices on the boundary of F, define

$$P(F,b) = \langle P_{w_1}, P_{w_2} \rangle \cap \langle \{P_w : w \in N(b) \setminus \{w_1, w_2\}\} \rangle \tag{2.3}$$

where $\langle \cdot \rangle$ denotes the affine span of a set of points. If b has degree d then by the the preceding discussion the right hand side is a transverse intersection inside a $d-2$ space of a line and a $d-3$ space. So $P(F,w)$ is indeed a point.

Proposition 2.4. *If F is a quadrilateral face with vertices w_1, w_2 and b_1, b_2 then urban renewal at F constructs the point $P(F,b_i)$ at the new white vertex closer to b_i for $i = 1, 2$.*

Proof. It suffices to show that $P(F,b_1)$ is the class of $v(F,b_1)$ in projective space (and similarly for $P(F,b_2)$ and $v(F,b_2)$). By definition, $v(F,b_1)$ is the linear combination of v_{w_1} and v_{w_2} appearing in R_{b_1}. Applying R_{b_1}, one can equivalently express $v(F,b_1)$ as a linear combination of $\{v_w : w \in N(b_1) \setminus \{w_1, w_2\}\}$. We get that $v(F,b_1)$ is on the intersection of two subspaces in a way that exactly projectivizes to the formula (2.3). □

Proposition 2.5. *Consider a degree 2 vertex addition move from G to G'. If the added degree 2 vertex b is black then the point P at the white vertex of G that got split is placed at both neighbors of b in G'. If the added degree 2 vertex w is white, let $P_1, \dots, P_k$ and $Q_1, \dots, Q_l$ be the points at the neighbors of the black vertex of G that got split, following the template of the bottom of Figure 3. Then the new point that gets placed at w is*

$$\langle P_1, \dots, P_k \rangle \cap \langle Q_1, \dots, Q_l \rangle.$$

Proof. The black degree 2 vertex addition case follows directly from the definitions. The proof in the white case follows the same approach as the proof of Proposition 2.4. □

To sum up, for each planar bipartite graph G we have a projective geometric dynamical system dictated by the corresponding dimer model. The state of the system is given by a choice of a point in projective space at each white vertex so that the points neighboring each black vertex form a circuit. The points (and the graph) evolve under local transformations, the most interesting of which is urban renewal as described by Proposition 2.4 and formula (2.3).

We will see that many systems, some in the pentagram map family some not, fit in this framework. For each such system we get for free the set of face weights Y_F and their corresponding evolution equations as in Proposition 2.2. These variables are easy to define in a projectively natural way. Suppose points $P_1, \dots, P_{2k}$ in an affine space are given with the triples $\{P_1, P_2, P_3\}$, $\{P_3, P_4, P_5\}$, $\dots$, $\{P_{2k-1}, P_{2k}, P_1\}$ all collinear. The *multi-ratio* (called a *cross ratio* for $k = 2$ and a *triple ratio* for $k = 3$) of the points is

$$[P_1, \dots, P_{2k}] = \frac{P_1 - P_2}{P_2 - P_3} \frac{P_3 - P_4}{P_4 - P_5} \cdots \frac{P_{2k-1} - P_{2k}}{P_{2k} - P_1}.$$

Each individual fraction involves 3 points on a line and is interpreted as a ratio of signed distances.

Proposition 2.6. *Let F be a face with boundary cycle $w_1, b_1, w_2, b_2, \dots, w_m, b_m$ in clockwise order. In terms of the points P_w, the face weight of F equals*

$$Y_F = (-1)^{m-1}[P_{w_1}, P(F, b_1), P_{w_2}, P(F, b_2), \dots, P_{w_m}, P(F, b_m)]^{-1}.$$

Proof. By definition we have lifts v_{w_i} of P_{w_i} and $v(F, b_i)$ of $P(F, b_i)$ such that

$$v(F, b_i) = K_{b_i w_i} v_{w_i} + K_{b_i w_{i+1}} v_{w_{i+1}}.$$

Applying gauge we can assume all $2m$ of these vectors lie in some affine hyperplane from which it follows that

$$1 = K_{b_i w_i} + K_{b_i w_{i+1}}.$$

As such the above can be rewritten

$$K_{b_i w_{i+1}}(v(F, b_i) - v_{w_{i+1}}) = K_{b_i w_i}(v_{w_i} - v(F, b_i)).$$

Viewing the P's as points on the hyperplane this shows

$$\frac{P(F, b_i) - P_{w_{i+1}}}{P_{w_i} - P(F, b_i)} = \frac{K_{b_i w_i}}{K_{b_i w_{i+1}}}.$$

Multiplying across all i produces the reciprocal of the multi-ratio on the left and the defining expression (2.2) for the face weights on the right. □

3. Examples

In this section, we consider several projective geometric systems from the literature, and explain how they fit in our framework. For each we identify the appropriate bipartite graph as well as the sequence of local transformations realizing the system. In some cases we also explicitly work out the associated dynamics on the face weights.

3.1. **The pentagram family.**

Example 3.1. The Laplace-Darboux system [4] operates on a 2-dimensional array of points in $\mathbb{P}^3$ for which the points of each primitive square are coplanar. It is convenient to index the points as $P_{i,j}$ for $i, j \in \mathbb{Z}$ with $i + j$ even. The centers of the squares are then (i, j) with $i + j$ odd so the condition is

$$P_{i,j-1}, P_{i-1,j}, P_{i+1,j}, P_{i,j+1} \text{ coplanar for } i + j \text{ odd}. \tag{3.1}$$

The system produces a new array of points $Q_{i,j}$ for $i + j$ odd defined by

$$Q_{i,j} = \langle P_{i,j-1}, P_{i+1,j} \rangle \cap \langle P_{i-1,j}, P_{i,j+1} \rangle.$$

To state Laplace-Darboux dynamics in our language take the infinite square grid graph $G = (\mathbb{Z}^2, E)$, which is bipartite with white vertices being those (i, j) with $i + j$ even. Place the points $P_{i,j}$ above at the white vertices. For each black vertex (i, j) with $i + j$ odd, the circuit condition says that the 4 neighboring points should be coplanar, which is precisely (3.1).

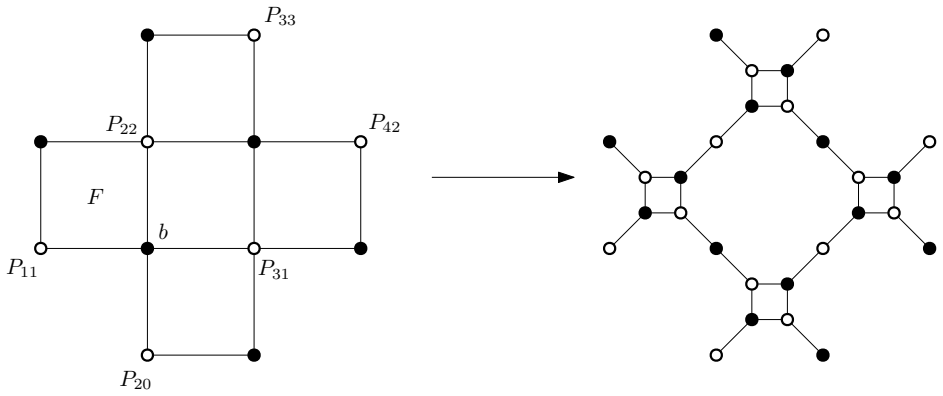

FIGURE 6. The local transformations which, when followed by degree 2 vertex removals, realize Laplace-Darboux dynamics.

To evolve the system, perform urban renewal at each face whose upper left corner is black. Figure 6 shows a local picture. Taking F, b as in the picture, one of the new points is

$$P(F,b) = \langle P_{2,0}, P_{3,1}\rangle \cap \langle P_{1,1}, P_{2,2}\rangle = Q_{2,1}.$$

Eliminating all degree 2 vertices in the resulting picture recovers the square lattice except with the colors of vertices reversed. The surviving points are precisely the $Q_{i,j}$.

Example 3.2. The pentagram map inputs a polygon in the plane with vertices A_i for $i \in \mathbb{Z}$ and outputs the polygon with vertices

$$B_i = \langle A_{i-1}, A_{i+1}\rangle \cap \langle A_i, A_{i+2}\rangle.$$

This operation can be seen as a reduction of Laplace-Darboux dynamics. Indeed, one can check that letting

$$P_{i,j} = A_{(i+3j)/2},\ i+j \text{ even}$$
$$Q_{i,j} = B_{(i+3j-1)/2},\ i+j \text{ odd}$$

gives an input-output pair for Laplace-Darboux. Note that $P_{i,j} = P_{i-3,j+1}$ and moreover if A is a closed n-gon meaning $A_{i+n} = A_i$ then $P_{i,j} = P_{i+2n,j}$.

As the bipartite graph for Laplace-Darboux was the square grid on $\mathbb{Z}^2$, the correct choice for the pentagram map is its quotient of this graph by the lattice generated by $(-3,1)$ and $(2n,0)$. This is a bipartite graph on a torus. Point A_i live at the vertex (equal to the class of) $(2i,0)$. The relations are of the form $A_{i-1}, A_i, A_{i+1}, A_{i+2}$ coplanar which explains why the whole configuration must be in a plane. Finally, the local transformations take the same form as for Laplace-Darboux.

The face weights of a polygon are precisely the y-parameters as defined in [11]. As an example, Figure 7 gives a portion of the bipartite graph. Applying Proposition 2.6, the variable at the face labeled F is

$$Y_F = -[A_3, \langle A_3, A_4\rangle \cap \langle A_1, A_2\rangle, A_4, \langle A_3, A_4\rangle \cap \langle A_5, A_6\rangle]^{-1}.$$

Although this algebraic formulation of the pentagram map was known, there may be other insights to be gained from the vector-relation perspective. For instance, if nearby vertices of a polygon come together it creates a singularity for the pentagram map dynamics. Keeping track of the coefficients of the relation satisfied by the points as they come together would be one way to try to control the behavior through the singularity.

Example 3.3. Different ways of putting the square grid graph on the torus produce different interesting systems. The higher pentagram map of Gekhtman et al. is obtained by working in $\mathbb{RP}^d$ and identifying (i,j) with $(i-d-1, j+d-1)$. Indeed, the $(-i,i)$ form a set of representatives of the white vertices. Placing a point P_i at each $(-i,i)$, the neighbors of a given black vertex are labeled by $P_i, P_{i+1}, P_{i+d}, P_{i+d+1}$. The condition that such four-tuples be coplanar is called the corrugated property and the resulting dynamics produces points

$$\langle P_i, P_{i+d}\rangle \cap \langle P_{i+1}, P_{i+d+1}\rangle$$

as in the higher pentagram map.

Example 3.4. The left of Figure 8 depicts one step of a certain pentagram spiral system. The input is a *seed* consisting of five points $A_1, \ldots, A_5$ with A_5 lying on the line through A_1 and A_4. The output is a new seed $A_2, \ldots, A_6$ with $A_6 = \langle A_1, A_3\rangle \cap \langle A_2, A_5\rangle$. If iterated the result is a polygonal curve that spirals inwards indefinitely.

The right of Figure 8 shows a bipartite graph whose vector-relation dynamics capture this system. As with the pentagram map on hexagons, the vertex set of the graph G is $\mathbb{Z}^2$ modded out by the lattice generated by $(-3,1)$ and $(12,0)$. However, G does not include all of the edges from the square grid. The figure shows exactly

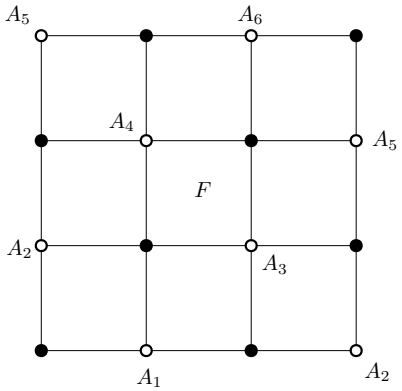

FIGURE 7. A portion of the bipartite graph whose vector-relation dynamics coincide with the pentagram map.

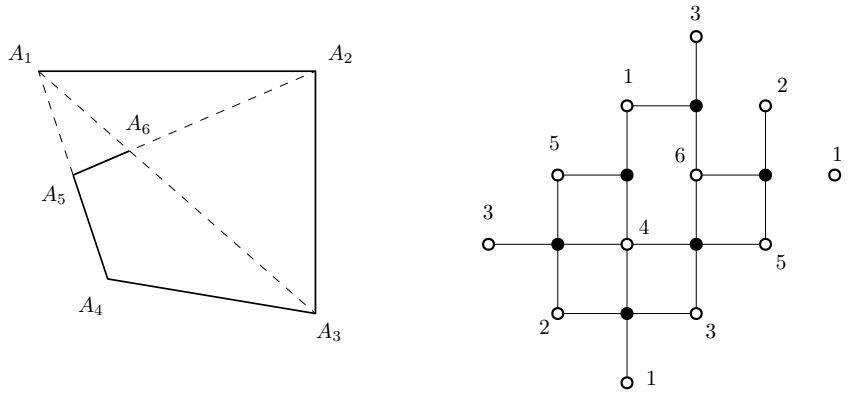

FIGURE 8. One step of a system that produces a pentagram spiral (left) along with the associated bipartite graph (right).

one copy of each edge and each black vertex, while the repeats among white vertices help to visualize how the picture repeats when lifted to $\mathbb{Z}^2$.

Place points A_i for $i = 1, \ldots, 6$ at the white vertices. There are three degree 4 black vertices which give conditions that $\{A_1, A_2, A_3, A_4\}$, $\{A_2, A_3, A_4, A_5\}$, and $\{A_3, A_4, A_5, A_6\}$ are coplanar. As such, all six points are on a common plane. There are also three degree 3 black vertices implying that the triples $\{A_1, A_4, A_5\}$, $\{A_1, A_3, A_6\}$, and $\{A_2, A_5, A_6\}$ are collinear. These match the defining conditions of the six points in the left picture. In short, being a configuration on G is equivalent to being a union of two consecutive seeds of the pentagram spiral.

We give a quick description of how to realize spiral dynamics. There is a quadrilateral face of G containing white vertices 1 and 3. Urban renewal at this face followed by a degree 2 vertex removal will produce a graph isomorphic to G. The points $A_2, \ldots, A_6$ will remain and there will also be a new point $A_7 = \langle A_1, A_3\rangle \cap \langle A_2, A_4\rangle$, which is the next point on the spiral. So the dynamics on the graph are equivalent to the spiral map, with the only discrepancy being that the former keeps track of six consecutive points at each time instead of five.

The graph G is a special case of the dual graph to a Gale-Robinson quiver. It is likely that every sufficiently large such graph models some combinatorial type of pentagram spiral.

Example 3.5. A Y-mesh is a map $(i, j) \to P_{i,j}$ from $\mathbb{Z}^2$ to a projective space such that each translate of a fixed 4 element subset of $\mathbb{Z}^2$ maps to a quadruple of collinear points. The second and third authors [12] defined a family of dynamical systems that iteratively build Y-meshes of various types. Each system can be described in terms of mutations of a quiver on a torus [12, Section 12]. We strongly suspect that vector-relation dynamics on the dual bipartite graph recover the original system. The only challenge is determining the correspondence between points of the Y-mesh and white vertices of the graph. We focus here on a single illustrative example.

The *rabbit map* acts on the space of triples A, B, C of polygons in $\mathbb{P}^4$ satisfying the conditions

$$A_{i-1}, B_{i+1}, C_i \text{ collinear}$$
$$A_{i+1}, B_i, C_i \text{ collinear}$$
$$A_{i-1}, B_{i-1}, B_{i+1}, C_{i+1} \text{ coplanar}$$

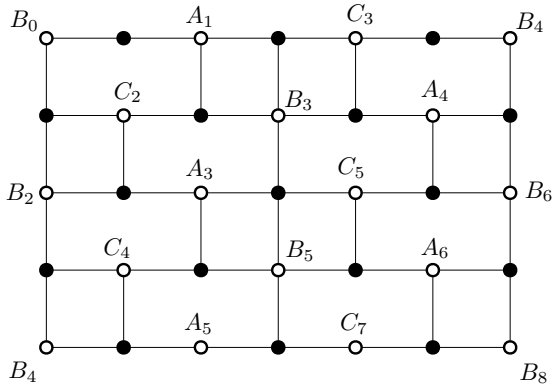

FIGURE 9. The bipartite graph corresponding to the rabbit map. The figure continues infinitely up and down, while the left and right sides are identified as per the labeling.

for all $i \in \mathbb{Z}$. The map takes (A, B, C) to (B, C, D) where

$$D_i = \langle A_{i-1}, B_{i+1} \rangle \cap \langle B_{i-1}, C_{i+1} \rangle$$

for all i. Each quadruple $A_{i-1}, B_{i+1}, C_i, D_i$ of points is collinear, indicating the type of the Y-mesh that this system constructs.

The vector-relation formulation of the rabbit map is given in Figure 9. The black vertices correspond exactly to the conditions listed above. Propagation is carried out by applying urban renewal for each i at the square face containing both A_{i-1} and B_{i+1}.

In general, the bipartite graph perspective represents a significant improvement in our understanding of Y-meshes. As an example, in the original formulation only the cross ratio y-variables are easy to describe and the others require a messy case by case analysis [12, Section 13]. Now we get a uniform description of all y-variables via Proposition 2.6. For instance, the hexagon in Figure 9 containing A_3, C_2, B_3 has weight

$$y_F = [A_3, B_2, C_2, A_1, B_3, \langle A_3, B_3 \rangle \cap \langle B_5, C_5 \rangle]^{-1}.$$

A central question that is open in general is what minimum collections of points determine the Y-mesh and what relations they satisfy (see [12, Section 8] for many examples including the rabbit case). There is hope that these questions have answers in terms of graph theoretic properties of G. A result of this flavor in a different context is given in Proposition 4.11.

3.2. **Q-nets.** Discrete conjugate nets, or *Q-nets* were introduced by Doliwa-Santini [5]; we follow the exposition of Bobenko-Suris [3]. We shall specifically be concerned with 3-dimensional Q-nets, defined as follows.

Definition 3.6. [3, Definition 2.1] A map $f : \mathbb{Z}^3 \to \mathbb{R}^3$ is a 3-dimensional Q-net in $\mathbb{R}^3$ if for every $u \in \mathbb{Z}^3$ and for every pair of indices $i, j \in \{1, 2, 3\}$ points $f(u), f(u + e_i), f(u + e_j), f(u + e_i + e_j)$ are coplanar (where e_1, e_2, e_3 are the generators of $\mathbb{Z}^3$).

While a Q-net is a static object, it is often convenient to think of it in a dynamical way as follows. For $u = (i, j, k)$ let $|u| = i + j + k$. A *generation* of vertices of a Q-net is the set of all $f(u)$ where $|u| = t$. Let us denote f_t such t-th generation. Then knowing f_t and f_{t+1} one can construct the next generation f_{t+2} as follows. Consider an elementary cube consisting of eight points $f(u + \varepsilon_1 e_1 + \varepsilon_2 e_2 + \varepsilon_3 e_3)$, where each ε_i is either 0 or 1. Assume $|u| = t - 1$. Then using the six points that belong to f_t, f_{t+1} one can construct three planes that have to contain $f(u + e_1 + e_2 + e_3) \in f_{t+2}$. Intersecting those planes we generically get the unique candidate for $f(u + e_1 + e_2 + e_3)$.

The problem of analytic description, which also can be called parametrization of Q-nets is discussed in [3], with first such description going back to the original work [5]. Our constructions suggests a new way to parametrize 3-dimensional Q-nets. Furthermore, since our parameters are cross-ratios of quadruples of points, it is natural to view it as parametrizing *projective Q-nets*, i.e. Q-nets considered up to projective equivalence.

Consider three consecutive generations f_t, f_{t+1}, f_{t+2} of a Q-net f. Their vertices and the edges that connect them can be conveniently visualized as a lozenge tiling dual to the Kagome lattice, see Figure 10. Vertices of each lozenge map into vertices of a face of one of the elementary cubes of a Q-net, and thus are coplanar. Thus, the geometry of the three generations of points is captured by the bipartite graph we get by placing a white vertex at each vertex of the lozenge tiling, and a black vertex at each face, see Figure 10. The set of points of this configuration is sufficient initial data to determine the whole Q-net. In fact, the rest of the Q-net is obtained via local transformations, which by an inductive argument boils down to the following.

Proposition 3.7. *The sequence of square moves shown in Figure 11 realizes geometrically a step of time evolution of the Q-net transitioning from vertex D to vertex D' of one of the elementary cubes.*

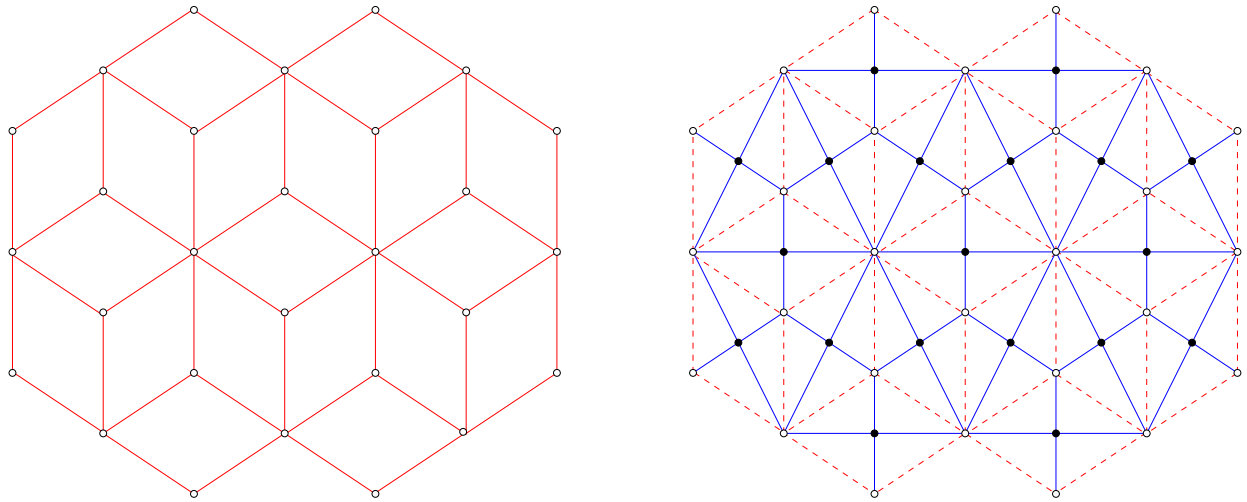

FIGURE 10. Three generations of a Q-net and the associated bipartite graph

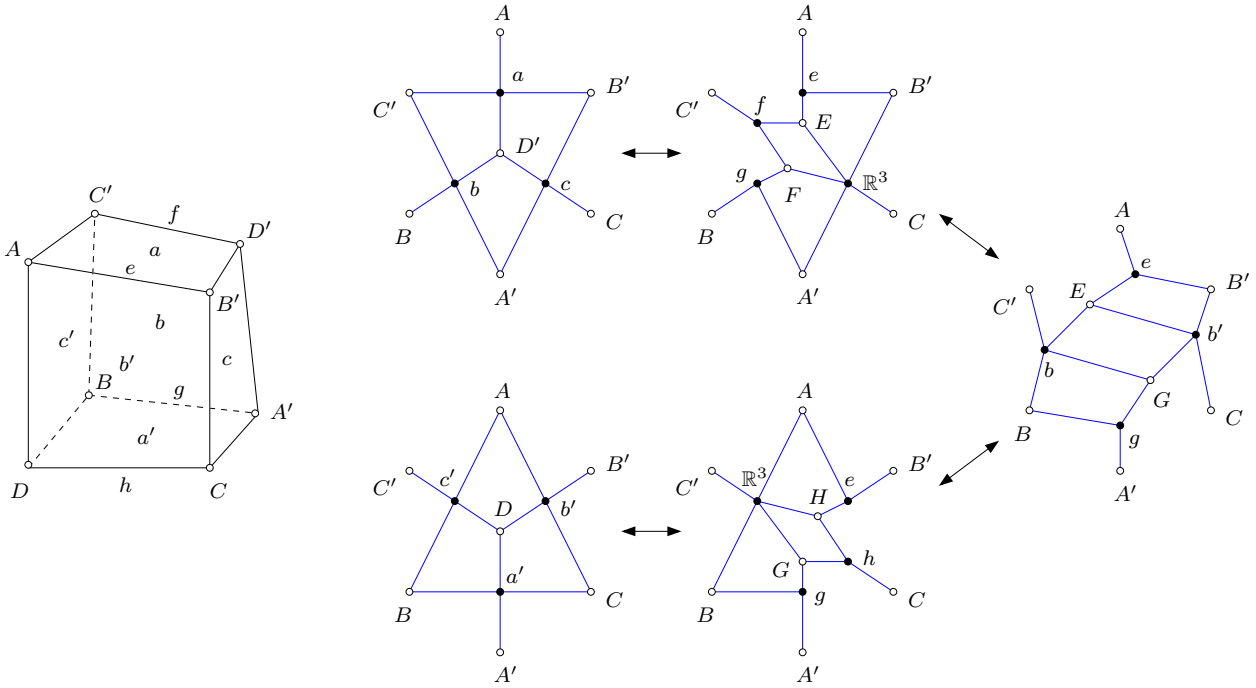

FIGURE 11. The gentrification sequence of moves. For convenience, each black vertex is labeled by the affine hull of the points at neighboring white vertices.

Proof. We verify the sequence of square moves using Proposition 2.4 on each step. For example, points G and H are formed by intersecting line CD with affine spans of the rest of black points surrounding respectively a' and b', i.e. with lines BA' and AB'. Here $E = C'D' \cap AB'$, $F = C'D' \cap BA'$, $G = A'B \cap CD$, $H = AB' \cap CD$, $a = \langle AB'D'C' \rangle$, $b = \langle A'BC'D' \rangle$, $c = \langle B'CA'D' \rangle$, $e = AB'$, $f = C'D'$, $g = A'B$, $h = CD$, $a' = \langle A'BDC \rangle$, $b' = \langle AB'CD \rangle$, $c' = \langle ADBC' \rangle$. □

Remark 3.8. This sequence of square moves has appeared in [15, Figure 8], without the current geometric interpretation, and under the name of *star-triangle move*. Here we introduce the name *gentrification* to emphasize its similar, but not coinciding nature with *superurban renewal* of [17], see below.

Denote $Q_{i,j,k}$ the vertex of the Q-net with coordinates i, j, k, and denote $Q^x_{i,j,k}$ the edge pointing from this vertex in the x direction, i.e. the edge connecting $Q_{i,j,k}$ with $Q_{i+1,j,k}$. Same for $Q^y_{i,j,k}$ and $Q^z_{i,j,k}$. The vertices of the tiling on the left of Figure 10 are home to three generations of the Q-net, say f_t, f_{t+1}, f_{t+2}. As such the edges correspond to the $Q^*_{i,j,k}$ with $i + j + k \in \{t, t + 1\}$ and $* \in \{x, y, z\}$. Meanwhile, the faces of the bipartite graph correspond to the edges of the tiling, with each edge connecting the two white vertices of the corresponding face. Each face is a quadrilateral with both of its black vertices having degree four. It follows from Proposition 2.6 that the face variable equals a negated cross ratio with two points being the endpoints

of the edge and the others being intersections of the edge with nearby parallel edges of the tiling. The exact formula depends on whether the edge connects f_t with f_{t+1} or f_{t+1} with f_{t+2}. To this end, define

$$Y^x_{i,j,k} = -[Q_{i,j,k}, Q^x_{i,j,k} \cap Q^x_{i,j+1,k}, Q_{i+1,j,k}, Q^x_{i,j,k} \cap Q^x_{i,j,k+1}]^{-1}$$
$$\widetilde{Y}^x_{i,j,k} = -[Q_{i,j,k}, Q^x_{i,j,k} \cap Q^x_{i,j,k-1}, Q_{i+1,j,k}, Q^x_{i,j,k} \cap Q^x_{i,j-1,k}]^{-1}$$

The formulas for the variables at y and z edges are obtained from these by performing a cyclic shift of subscripts and a substitution $x \to y \to z \to x$ of superscripts.

Proposition 3.9. *The collection of face weights, also known as the Y-seed, corresponding to the above setup is*

$$\{Y^*_{i,j,k} : i+j+k = t\} \cup \{\widetilde{Y}^*_{i,j,k} : i+j+k = t+1\}.$$

Proposition 3.10. *The variables Y evolve according to the following formulas (and their cyclic shifts):*

$$\widetilde{Y}^x_{i,j+1,k+1} = (Y^y_{i,j,k})^{-1} \frac{1 + Y^x_{i,j,k} + Y^y_{i,j,k} Y^x_{i,j,k}}{1 + Y^z_{i,j,k} + Y^z_{i,j,k} Y^x_{i,j,k}}$$
$$Y^x_{i+1,j,k} = \widetilde{Y}^x_{i+1,j,k} Y^x_{i+1,j-1,k} Y^y_{i+1,j-1,k} \frac{1 + Y^z_{i+1,j,k-1} + Y^z_{i+1,j,k-1} Y^x_{i+1,j,k-1}}{1 + Y^x_{i+1,j-1,k} + Y^x_{i+1,j-1,k} Y^y_{i+1,j-1,k}}$$

for all $i+j+k = t$.

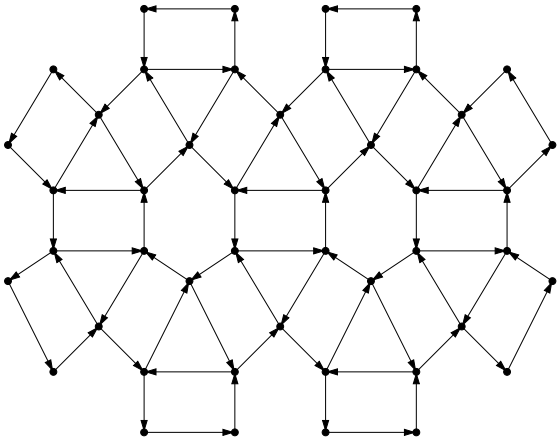

FIGURE 12. Q-net quiver.

Proof. One simply follows Y-variable dynamics of the associated cluster algebra, whose quiver is shown in Figure 12. □

Remark 3.11. There is of course also X-variable cluster dynamics associated with gentrification. Its given by

$$X^x_{i,j+1,k+1} = \frac{X^x_{i,j,k} X^z_{i,j+1,k} X^y_{i,j,k+1} + X^y_{i,j,k} X^z_{i,j+1,k} X^x_{i,j,k+1} + X^z_{i,j,k} X^x_{i,j+1,k} X^y_{i,j,k+1}}{X^y_{i,j,k} X^z_{i,j,k}}.$$

It is not clear if the X-variables have any geometric meaning in terms of Q-nets however.

Remark 3.12. Several cluster algebra descriptions of geometric systems, including Q-nets and discrete Darboux maps, were found independently in collaboration with Fu [2]. A common situation that in particular holds for Q-nets is that there are two distinct sets of geometric quantities that each evolve according to the (coefficient type) dynamics of the same quiver. One of the goals of [2] is to better understand this phenomenon.

3.3. **Discrete Darboux maps.** Discrete Darboux maps were introduced by Schief [27]; we follow the exposition of Bobenko-Suris [3, Exercise 2.8, 2.9]. We identify the set of edges of a 3-dimensional cubic lattice with $\mathbb{Z}^3 \times \{x, y, z\}$ in that each edge is in bijection with a node of $\mathbb{Z}^3$ and one of the three positive directions x, y, z in which the edge points from that node.

Definition 3.13. [3, Definition 2.1] A map $f : \mathbb{Z}^3 \times \{x, y, z\} \to \mathbb{R}^3$ is a 3-dimensional discrete Darboux map if for every face of the cubic lattice the images of its edges are collinear. In other words,

$$f^x_{i,j,k}, f^y_{i,j,k}, f^x_{i,j+1,k}, f^y_{i+1,j,k} \text{ are collinear,}$$
$$f^x_{i,j,k}, f^z_{i,j,k}, f^x_{i,j,k+1}, f^z_{i+1,j,k} \text{ are collinear,}$$
$$f^y_{i,j,k}, f^z_{i,j,k}, f^z_{i,j+1,k}, f^y_{i,j,k+1} \text{ are collinear.}$$

Remark 3.14. In Schief's definition [27] the function takes values on faces of a cubic lattice, not edges. However, as Schief himself observes in loc. cit. the two are equivalent since one can consider a dual cubic lattice with vertices corresponding to elementary cubes of the original one.

One can think of discrete Darboux maps in a dynamical way in a similar fashion to Q-nets. Define the generation of an edge in $\mathbb{Z}^3 \times \{x, y, z\}$ as the sum of its three coordinates. Then it is easy to see, as pointed out in [3, Exercice 2.8], that each generation determines the next one uniquely. For example, $f^z_{i+1,j+1,k}$ is the intersection of the line connecting $f^y_{i+1,j,k}$ to $f^z_{i+1,j,k}$ with the line connecting $f^x_{i,j+1,k}$ to $f^z_{i,j+1,k}$. The fact that six points $f^y_{i+1,j,k}$, $f^z_{i+1,j,k}$, $f^x_{i,j+1,k}$, $f^z_{i,j+1,k}$, $f^x_{i,j,k+1}$, and $f^y_{i,j,k+1}$ lie in one plane is a necessarily condition that is easily seen to self-propagate.

The geometry of a discrete Darboux map is captured by the bipartite graph in Figure 13. Here on each edge of the lozenge tiling we place a white vertex signifying a point. To force the four points on the sides of a single lozenge to lie on one line we introduce two black vertices inside. It is clear that if the two triples of points lie on one line, then so do all four points. Figure 13 should be compared for example with [17, Figure 7].

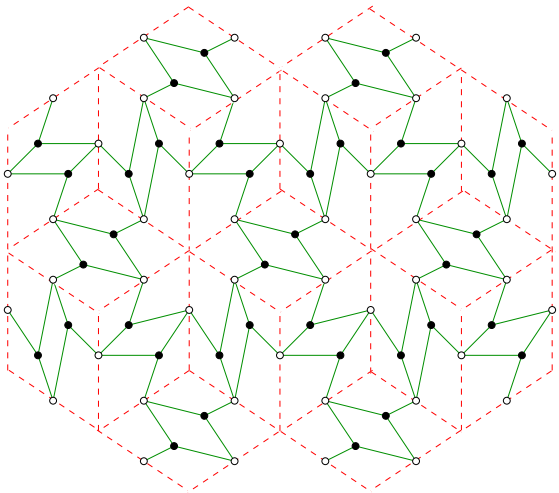

FIGURE 13. The bipartite graph of a discrete Darboux map

Proposition 3.15. *The sequence of square moves shown in Figure 14 realizes geometrically a step of time evolution of the discrete Darboux map transitioning from vertexes G, H, K to vertices L, M, N of the elementary hexahedron.*

Proof. We verify the sequence of square moves using Proposition 2.4 on each step. □

Remark 3.16. This sequence of square moves has appeared in [17, Figure 6], without the current geometric interpretation, under the name of *superurban renewal*.

Proposition 2.6 suggests we introduce the following variables, one for each region in Figure 13. For the variables associated with lozenges we get

$$Y^{xy}_{ijk} = -[f^x_{ijk}, f^y_{i+1,j,k}, f^x_{i,j+1,k}, f^y_{ijk}]^{-1},$$

and similar formulas for other pairs of indexes. The variables associated with vertices of lozenges come in three flavors, as there are three generations of them present in the picture.

$$\begin{aligned}
Y^{\text{in}}_{ijk} &= [f^x_{ijk}, f^y_{i+1,j,k}, f^y_{ijk}, f^z_{i,j+1,k}, f^z_{ijk}, f^x_{i,j,k+1}]^{-1}, \text{ for } i+j+k = t \\
Y^{\text{mid}}_{ijk} &= -[f^x_{ijk}, f^x_{i,j,k-1}, f^z_{i,j,k-1}, f^z_{i,j+1,k-1}, f^y_{ijk}, f^y_{i-1,j,k}, f^x_{i-1,j,k}, f^x_{i-1,j,k+1}, \\
&\qquad f^z_{ijk}, f^z_{i,j-1,k}, f^y_{i,j-1,k}, f^y_{i+1,j-1,k}]^{-1}, \text{ for } i+j+k = t+1 \\
Y^{\text{out}}_{ijk} &= [f^x_{i-1,j,k}, f^y_{i-1,j-1,k}, f^y_{i,j-1,k}, f^z_{i,j-1,k-1}, f^z_{i,j,k-1}, f^x_{i-1,j,k-1}]^{-1}, \text{ for } i+j+k = t+2.
\end{aligned}$$

The quiver is shown in Figure 15. The Y-s evolve according to the Y-dynamics formulas of the associated cluster algebra. The formulas are too long to be written here.

Remark 3.17. The X-variable dynamics associated with this quiver and sequence of mutations has appeared in [17, Lemma 2.3], see the formulas given there.

Remark 3.18. The notions of Q-nets and discrete Darboux maps are related by projective duality. As such, it is interesting that we get distinct quivers for these two systems. It is unclear if there is a good notion of projective duality on the level of vector-relation configurations in general.

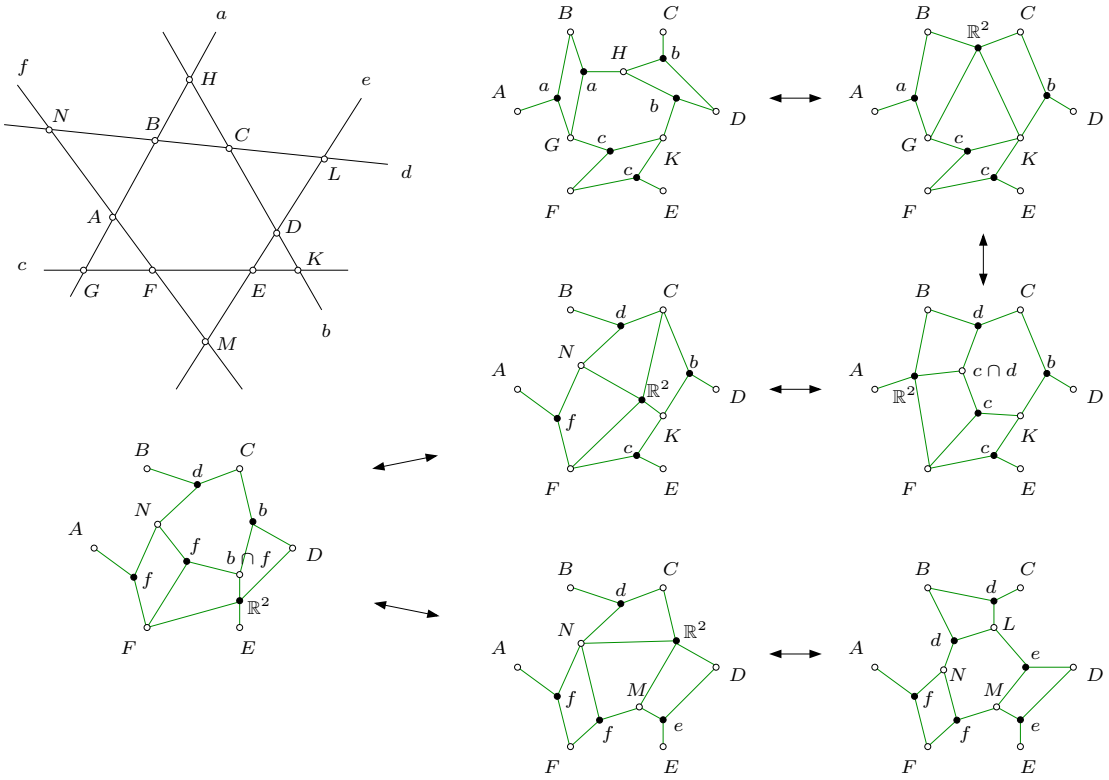

FIGURE 14. Superurban renewal.

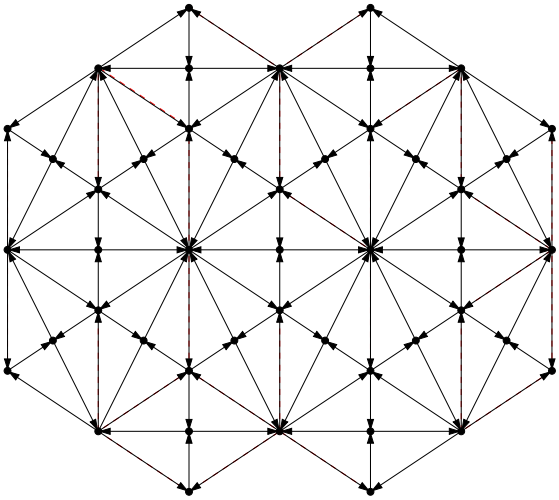

FIGURE 15. Discrete Darboux map quiver.

4. Configurations on plabic graphs

4.1. **Background on positroid varieties.** We now return to the plabic graph case. The proof of Theorem 1.5 utilizes a significant amount of the theory of positroid varieties. We begin by reviewing the relevant material, generally following [23] and [21].

The totally nonnegative Grassmannian is the set of $A \in Gr(k,n)$ for which $\Delta_J(A)$ is real and nonnegative for all J. The *matroid* of any $A \in Gr(k,n)$ is

$$\mathcal{M} = \{J : \Delta_J(A) \neq 0\}.$$

A *positroid* is a set of k-element subsets of $\{1,\dots,n\}$ that arises as the matroid of a point in the totally nonnegative Grassmannian. We also denote a positroid by $\mathcal{M}$ even though this is a more restrictive notion than a matroid.

Let $\mathcal{M}$ be a positroid. For $j = 1,\dots,n$, consider the column order $j < j+1 < \dots < n < 1 < \dots < j-1$. Let I_j be the lexicographically minimal element of $\mathcal{M}$ relative to this order. The collection of sets $(I_1,\dots,I_n)$ is called the *Grassmann necklace* of $\mathcal{M}$. The positroids index a decomposition of the complex Grassmannian by

open positroid varieties $\Pi^\circ_{\mathcal{M}}$, defined as intersections of cyclic shifts of Schubert cells encoded by $(I_1, \ldots, I_n)$. The *positroid variety* $\Pi_{\mathcal{M}}$ is defined to be the Zariski closure of $\Pi^\circ_{\mathcal{M}}$. In order to give quicker definitions, we fall back on the literature.

Theorem 4.1 (Knutson–Lam–Speyer [19])**.** *The positroid variety* $\Pi_{\mathcal{M}}$ *is a closed irreducible variety defined in the Grassmannian by*

$$\Pi_{\mathcal{M}} = \{A \in Gr_{k,n} : \Delta_J(A) = 0 \text{ for all } J \notin \mathcal{M}\}.$$

Taking this result as given we can define $\Pi^\circ_{\mathcal{M}}$ as the set of $A \in \Pi_{\mathcal{M}}$ whose Plücker coordinates $\Delta_{I_j}(A)$ coming from the Grassmann necklace are all nonzero.

Let $G = (B \cup W, E)$ be a plabic graph. Following our conventions, all boundary vertices are white. Let n be the number of boundary vertices and $k = |W| - |B|$. An almost perfect matching is a matching in G that uses all internal vertices. Hence it is a matching of B with $W \setminus J$ where $J \subseteq \{1, \ldots, n\}$ (identified with the boundary vertices) and $|J| = k$. The *positroid* of G, denoted $\mathcal{M}_G$ is the set of J that arise this way as the unused vertices of an almost perfect matching.

The *boundary measurement map* is a function that inputs a set of nonzero edge weights on G and outputs a point $A \in \Pi^\circ_{\mathcal{M}}$, where $\mathcal{M} = \mathcal{M}_G$. If $\mathrm{wt} : E \to \mathbb{C}^*$ is the weight function then A is defined by its Plücker coordinates via

$$\Delta_J(A) = \sum_{\pi} \prod_{e \in \pi} \mathrm{wt}(e) \tag{4.1}$$

where the sum is over matchings π of B with $W \setminus J$. The result is unchanged by gauge transformations at internal vertices. The boundary measurement map plays a key role in the study of the nonnegative Grassmannian as it proves that the individual strata therein are cells.

The situation is more complicated in the complex case as the boundary measurement map is not surjective. Its image, which will play a key role for us, was identified by Muller and Speyer [23]. First, they define a remarkable isomorphism $\tau : \Pi^\circ_{\mathcal{M}} \to \Pi^\circ_{\mathcal{M}}$ called the *right twist*. Suppose $A = [v_1 \cdots v_n]$ and $\tau(A) = [v'_1 \cdots v'_n]$. We do not give the full definition of the twist, but instead state a key property (that defines the v'_j up to scale). Specifically for each j, v'_j is orthogonal to v_i for all $i \in I_j \setminus \{j\}$.

The last piece of technology we need, both in relation to the boundary measurement map and for other purposes, is the notion of zigzag paths in G. A *zigzag path* is a path of G that turns maximally left (respectively right) at each white (respectively black) vertex and either starts and ends at the boundary or is an internal cycle. Each directed edge can be extended to a zigzag path, so there are two zigzag paths through each edge. Define an *intersection* of two zigzags to be such an edge that they traverse in opposite directions. Say that G is *reduced* if

- each zigzag path starts and ends at the boundary,
- each zigzag of length greater than two has no self intersections
- no pair of distinct zigzags have a pair of intersections that they encounter in the same order.

If G is reduced then there are exactly n zigzags, one starting at each boundary vertex. Call j the number of the zigzag starting at vertex j. A zigzag that does not self intersect divides the disk into two regions. For F a face of G, let S_F denote the set of j for which F lies to the left of zigzag number j. There are two corner cases. If j is attached to a degree 1 black vertex b then zigzag j goes from j to b and back to j. In this event all faces are considered to be to the right of the zigzag. On the other hand, if j is an isolated boundary vertex then zigzag j is an empty path that all faces are considered to lie to the left of. With these conventions one can show that all S_F have size k.

Theorem 4.2 (Muller-Speyer [23])**.** *The image of the boundary measurement map is the set of* $A \in \Pi^\circ_{\mathcal{M}}$ *whose twist* $A' = \tau(A)$ *satisfies*

$$\Delta_{S_F}(A') \neq 0$$

for all faces F *of* G*. This set is dense in* $\Pi^\circ_{\mathcal{M}}$ *and in fact the coordinates* $\Delta_{S_F}(A')$ *give it the structure of an algebraic torus.*

4.2. **Sharpening the main result.** The remainder of this section is devoted to the proof of Theorem 1.5, and we begin by reformulating and sharpening this result. Let $G = (B \cup W, E)$ be a plabic graph with all the notation of Section 1.2. Recall in this setting we only allow gauge transformations at the internal vertices. Let $\mathcal{C}_G$ denote the space of gauge equivalence classes of vector-relation configurations on G modulo the action of $GL_k(\mathbb{C})$.

If $(\mathbf{v}, \mathbf{R}) \in \mathcal{C}_G$ then by assumption $v_1, \ldots, v_n$ span $V = \mathbb{C}^k$. The v_i are defined up to a common change of basis so $A = [v_1 \cdots v_n]$ is a well-defined point of $Gr_{k,n}$. We use Φ to denote the map $\Phi : \mathcal{C}_G \to Gr_{k,n}$ taking $(\mathbf{v}, \mathbf{R})$ to A, and we call Φ the *boundary restriction map*.

In this language, Theorem 1.5 asserts that Φ maps into $\Pi_{\mathcal{M}}$ and that generic points in this positroid variety have unique preimages. Let T_G be the image of the boundary measurement map. We will show that elements of T_G are sufficiently generic for this purpose. By Theorem 4.2, T_G is dense in $\Pi^\circ_{\mathcal{M}}$ which in turn is dense in $\Pi_{\mathcal{M}}$.

It is also simple to describe the set of preimages of the $A \in T_G$. Let $\mathcal{C}_G^\circ$ denote the set of $(\mathbf{v}, \mathbf{R}) \in \mathcal{C}_G$ for which $K_{bw} \neq 0$ whenever $\overline{bw} \in E$. There is a better characterization of $\mathcal{C}_G^\circ$ along the lines of the circuit condition discussed previously, but we delay this definition until we are in a better position to prove its equivalence.

We now state the stronger version of Theorem 1.5, which is the one we will prove.

Theorem 4.3. *Let G be a reduced plabic graph.*

(1) The image of Φ is contained in $\Pi_{\mathcal{M}}$.
(2) The restriction of Φ to $\mathcal{C}_G^\circ$ is an isomorphism with its image T_G.
(3) $\mathcal{C}_G^\circ = \Phi^{-1}(T_G)$.

4.3. **Connection to the boundary measurement map.** It turns out that an element of $\mathcal{C}_G$ is completely determined by its Kasteleyn matrix K. The potentially nonzero entries of K are in bijection with edges of G. As such, viewing K as the input of the boundary restriction map Φ gives it the same feel as the boundary measurement map. As in Section 2.1, we will eventually introduce certain signs to establish the exact relationship.

Lemma 4.4. *Let $\mathbf{v} \in \mathcal{C}_G$. There is a surjective linear map $\varphi : \mathbb{C}^N \to V$ with kernel equal to the row span $\operatorname{row}(K)$ such that each v_w is mapped to by the corresponding coordinate vector $e_w \in \mathbb{C}^N$.*

Proof. We can define a linear map φ via $\varphi(e_w) = v_w$ for all $w \in W$. As $v_1, \ldots, v_n$ span V, this map is surjective. Any given row of K is indexed by some $b \in B$, and equals $\sum_w K_{bw} e_w$. As such it gets mapped to $\sum_w K_{bw} v_w$ which equals zero by relation R_b. So $\operatorname{row}(K) \subseteq \ker(\varphi)$. But

$$\dim \operatorname{row}(K) = M$$

since K is full rank and

$$\dim \ker(\varphi) = N - \dim(V) = N - k = M$$

since φ is surjective so $\ker(\varphi) = \operatorname{row}(K)$. □

The previous establishes that a configuration in this setting is completely determined by K. More precisely, K determines a configuration in the ambient space $\mathbb{C}^N/\operatorname{row}(K)$ whose vectors are projections of the coordinate vectors and which is isomorphic to any other configuration giving rise to K.

Lemma 4.5. *Let $\mathbf{v} \in \mathcal{C}_G$ and let $S = \{w_1, \ldots, w_k\} \subseteq W$. Then*

$$\det[v_{w_1} \cdots v_{w_k}] = \pm\lambda \Delta_{W \setminus S}(K)$$

where λ is a nonzero scalar not depending on S and Δ_J denotes the determinant of a submatrix consisting of all rows and a specified set J of columns of a matrix.

Proof. By Lemma 4.4, $\mathbf{v}$ is isomorphic to the configuration of the projections of coordinate vectors in $U = \mathbb{R}^N/\operatorname{row}(K)$. There is a volume form on U defined by lifting $u_1, \ldots u_k \in U$ to (row) vectors in $\mathbb{R}^N$, placing them on top of K, and taking the determinant of the resulting $N \times N$ matrix. Applied to $e_{w_1}, \ldots, e_{w_k}$, the result equals $\pm\Delta_{W \setminus S}(K)$ (if S is in increasing order the sign is determined by the parity of $(w_1 - 1) + \ldots + (w_k - k)$). The isomorphism scales volume by some nonzero λ giving the formula for $\det[v_{w_1} \cdots v_{w_k}]$. □

Corollary 4.6. *Let $\mathbf{v} \in \mathcal{C}_G$ and $A = \Phi(\mathbf{v})$. Let $J = \{j_1, \ldots, j_k\}$ with $1 \leq j_1 < \ldots < j_k \leq n$. Then the Plücker coordinates of A are*

$$\Delta_J(A) = \pm\Delta_{W \setminus J}(K) \tag{4.2}$$

with the sign determined by the parity of $(j_1 - 1) + \ldots + (j_k - k)$.

Proof. A representing matrix for A is $[v_1 \cdots v_n]$, and we can compute its minors using Lemma 4.5. The Plücker coordinates are only defined up to multiplication by a common constant so we can ignore the λ's. □

Unfolding (4.2), we have

$$\Delta_J(A) = \pm \sum_f \operatorname{sgn}(f) \prod_{b \in B} K_{b, f(b)}$$

where the sum is over bijections f from B to $W \setminus J$. In fact $K_{bw} = 0$ unless $\overline{bw}$ is an edge, so we only get a nonzero terms if the set of $\overline{bf(b)}$ form an almost perfect matching of G avoiding the vertex set J. So we can rewrite the formula as

$$\Delta_J(A) = \pm \sum_\pi \operatorname{sgn}(\pi) \prod_{\overline{bw} \in \pi} K_{bw}, \tag{4.3}$$

the sum being over such matchings π. Aside from the signs, this formula has the exact same form as the defining equation (4.1) of the boundary measurement map.

To rectify these definitions, we introduce a version of Kasteleyn signs for plabic graphs. Let G be a plabic graph as above. By a *face* of G, we mean a connected component of the complement of the graph in the disk

in which it is embedded. A face is *internal* if its boundary is a closed walk in G and *external* otherwise. The boundary of an external face is an interlacing collection of walks in G and segments of the boundary of the disk. There is a unique boundary face including the boundary segment of the disk from n to 1. We call this face the *infinite face* and all other faces *finite faces*

Let $\varepsilon_{bw} = \pm 1$ for each edge $\overline{bw}$ of G. Say these constitute a choice of *Kasteleyn signs* if

- the product of the signs along the boundary of each internal $2m$-gon face is $(-1)^{m-1}$ and
- the product of the signs along the walk(s) on the boundary of each finite external face is $(-1)^{m+a-1}$, where a is the number of said walk(s) and $2m$ is the total number of edges along them.

Several notes are in order. Each walk on the boundary of an external face starts and ends at a boundary vertex and hence has even length as we assume boundary vertices are white. No assumption is made about the product of the signs around the infinite face. Lastly, the most common case is that G is connected. In that event each finite external face is cut out by a single ($a = 1$) path from i to $i+1$ and the second condition becomes that the product of signs along this path is $(-1)^m$ where $2m$ is its length.

Remark 4.7. One reference for Kasteleyn signs on plabic graphs is a short note of Speyer [29]. He does not directly identify the conditions above. Instead he defines the signs implicitly so that a certain result (along the lines of our Proposition 4.9) holds and then proves that such signs exist with a topological argument.

Proposition 4.8. *A choice of Kasteleyn signs on G exists.*

Proof. Extend G to a new graph $\widetilde{G}$ by adding a single black vertex b_∞ and n edges connecting b_∞ to the boundary vertices $1, \ldots, n$. Then $\widetilde{G}$ can be embedded in a sphere and the faces of $\widetilde{G}$ in the standard sense biject in a natural way with the faces of G as defined above. Consider the faces of $\widetilde{G}$ finite or infinite as dictated by this bijection. By ordinary Kasteleyn theory signs can be chosen on the edges of $\widetilde{G}$ so that each finite $2m$-gon face has a product of signs equal to $(-1)^{m-1}$. This property is preserved by gauge transformations wherein all signs adjacent to a given vertex are flipped. Applying gauge as needed at vertices 1 through n we can assume that all signs of edges adjacent to b_∞ are positive. Restricting the signs to the subgraph G yields precisely the right properties. □

Proposition 4.9. *Let $\mathbf{v} \in \mathcal{C}_G$ and suppose that all coefficients K_{bw} for $\overline{bw} \in E$ are nonzero. Define* $\mathrm{wt} : E \to \mathbb{C}^*$ *by* $\mathrm{wt}(\overline{bw}) = \varepsilon_{bw} K_{bw}$ *for a fixed choice of Kasteleyn signs. Then $\Phi(v)$ equals the output of the boundary measurement map applied to this weight function.*

Proof. Substitute $K_{bw} = \varepsilon_{bw}\mathrm{wt}(\overline{bw})$ into (4.3). Let $\varepsilon_J = \pm 1$ as per the sign in the front of the summation, which as previously mentioned is based on the parity of $(j_1 - 1) + \ldots + (j_k - k)$. So given J and a matching π of B with $W \setminus J$, the sign of the corresponding term is

$$\varepsilon_J \mathrm{sgn}(\pi) \prod_{\overline{bw} \in \pi} \varepsilon_{bw}. \tag{4.4}$$

To match (4.1) we need to show all these signs are equal (it is okay if they are all negative as the Plücker coordinates are only defined up to a common multiple). For two matchings with the same J this property is standard for Kasteleyn theory. One possible reference in [14, Theorem 2], and in fact we will follow the same outline in our proof of the general case.

We will compare the signs from (4.4) corresponding to the pair J_1, π_1 and the pair J_2, π_2. The disjoint union of the edges of π_1 and π_2 gives a multigraph for which each internal vertex has degree 2 and each boundary vertex has degree 0, 1, or 2. Each component (not counting isolated boundary vertices) is a doubled edge, a cycle, or a path starting and ending at the boundary. Each path and cycle alternates between edges of π_1 and π_2. Starting from π_1 one can *flip* along such a component by switching to the other half of the edges to obtain a matching with greater overlap with π_2. By induction it suffices to consider the case when π_1 and π_2 are related by a single flip. As already mentioned, the case of flipping a cycle in the graph is classical, so we focus on the path case.

Suppose π_1 and π_2 are related by a flip of a path from i to j with $i < j$. Without loss of generality, π_2 contains the edge of the path incident to i. It follows that $I_2 = I_1 \setminus \{i\} \cup \{j\}$. Therefore

$$\frac{\varepsilon_{I_2}}{\varepsilon_{I_1}} = (-1)^{j-i}. \tag{4.5}$$

We next consider the signs of the matchings. To make comparison easier, pass to the graph $\widetilde{G}$ from the proof of Proposition 4.8. Extend the matchings to $\widetilde{\pi}_1 = \pi_1 \cup \{\overline{ib_\infty}\}$ and $\widetilde{\pi}_2 = \pi_2 \cup \{\overline{jb_\infty}\}$. Both are matchings of $B \cup \{b_\infty\}$ with $W \setminus (I_1 \cap I_2)$. They are related by a flip in $\widetilde{G}$ about a cycle consisting of the original path from i to j along with the edges from i and j to b_∞. It follows that $\mathrm{sgn}(\widetilde{\pi}_2) = (-1)^{m-1}\mathrm{sgn}(\widetilde{\pi}_1)$ where $2m$ is the number of edges of this cycle. Now consider π_1 as an $M \times M$ permutation matrix with columns indexed by $W \setminus I_1$. Then $\widetilde{\pi}_1$ is obtained by adding a row to the end corresponding to b_∞, adding a column in the

appropriate place corresponding to i, and putting a 1 where the new row and column intersect. The columns right of the new one are indexed by $\{i+1,\dots,N\}\setminus I_1$, so

$$\operatorname{sgn}(\widetilde{\pi}_1) = (-1)^{|\{i+1,\dots,N\}\setminus I_1|}\operatorname{sgn}(\pi_1).$$

By a similar argument

$$\operatorname{sgn}(\widetilde{\pi}_2) = (-1)^{|\{j+1,\dots,N\}\setminus I_2|}\operatorname{sgn}(\pi_2).$$

Putting the pieces together

$$\frac{\operatorname{sgn}(\pi_2)}{\operatorname{sgn}(\pi_1)} = (-1)^{m-1+|\{i+1,\dots,j\}\setminus I_1|} \tag{4.6}$$

using the fact that I_1 and I_2 agree beyond j.

The last consideration is the sign coming from the weights on the edges where π_1 and π_2 differ, i.e. along the path from i to j. As in the previous paragraph we complete this to a cycle of length $2m$ passing through b_∞. This addition has no effect on signs because, as in the proof of Proposition 4.8 we take all edges adjacent to b_∞ to have sign $+1$. We have a cycle in $\widetilde{G}$, a graph with ordinary Kasteleyn signs, so by [14, Lemma 1] the signs around it come to $(-1)^{1+m+l}$ where l is the number of vertices properly inside the cycle, "inside" referring to the component that does not include the infinite face. By our conventions, this inside region includes the boundary vertices $i+1,\dots,j-1$ and not the others. Restricted to this region, the matching π_1 includes all vertices other than $\{i+1,\dots,j-1\}\cap I_1$. The vertices covered by π_1 come in pairs so l has the same parity as $|\{i+1,\dots,j-1\}\cap I_1|$. Therefore

$$\frac{\prod_{\overline{bw}\in\pi_2}\varepsilon_{bw}}{\prod_{\overline{bw}\in\pi_1}\varepsilon_{bw}} = (-1)^{1+m+|\{i+1,\dots,j-1\}\cap I_1|}. \tag{4.7}$$

Multiplying (4.5), (4.6), and (4.7), we get that the ratio of the signs of the two terms is governed by the parity of

$$2m+j-i+|\{i+1,\dots,j\}\setminus I_1|+|\{i+1,\dots,j-1\}\cap I_1|.$$

which equals $2m+j-i+j-i = 2(m+j-i)$ (using that $j\notin I_1$). This number is even so the terms have the same sign as desired.

□

Much, but not all, of Theorem 4.3 can be derived from analogous properties of the boundary measurement map. We will give largely self-contained proofs to demonstrate the power of our model and to suggest some new insights. Before moving on, we note that part 1 of Theorem 4.3 follows immediately from the results of this subsection.

Proposition 4.10. *If $\mathbf{v}\in\mathcal{C}_G$ then $\Phi(\mathbf{v})\in\Pi_{\mathcal{M}}$.*

Proof. Let $J\subseteq\{1,\dots,n\}$ with $|J|=k$ and suppose $J\notin\mathcal{M}$. By definition of $\mathcal{M}$ there is no almost perfect matching of G avoiding J. Therefore the sum in (4.3) is empty and we get $\Delta_J(\Phi(v))=0$. So $\Phi(v)$ satisfies the defining equations of $\Pi_{\mathcal{M}}$. □

The last result identifies linear dependent sets of size k among the boundary vectors. The result generalizes easily.

Proposition 4.11. *Let $\mathbf{v}\in\mathcal{C}_G$ and let $S\subseteq W$ be any set of white vertices. Suppose there is no matching of B with a subset of W disjoint from S. Then the vectors v_w for $w\in S$ are linearly dependent.*

Proof. First suppose $|S|=k$. Then the v_w for $w\in S$ form a square matrix whose determinant can be calculated using Lemma 4.5. There is no matching of B with $W\setminus S$ so the right hand side is zero and the vectors are dependent. If $|S|<k$ then we can augment S arbitrarily to get a set of size k satisfying the same hypotheses and hence corresponding to a dependent set. In other words $\{v_w : w\in S\}$ cannot be extended in the configuration to a basis of V. All vectors together span V so it follows that the set is dependent. □

Remark 4.12. Restricting to the $|S|=k$ case, one might hope for the stronger statement that $\{v_w : w\in S\}$ is a basis if and only if there is a matching of B with $W\setminus S$. The if direction only holds for generic $\mathbf{v}\in\mathcal{C}_G$. In the generic case, the matroid of the vectors of $\mathbf{v}$ is dual to the so-called *transversal matroid* of the bipartite graph G. This result is very similar to one of Lindström [22]. The similarity comes as no surprise as Lindström's famed lemma, which he introduced in that paper, is an essential ingredient in the boundary measurement map.

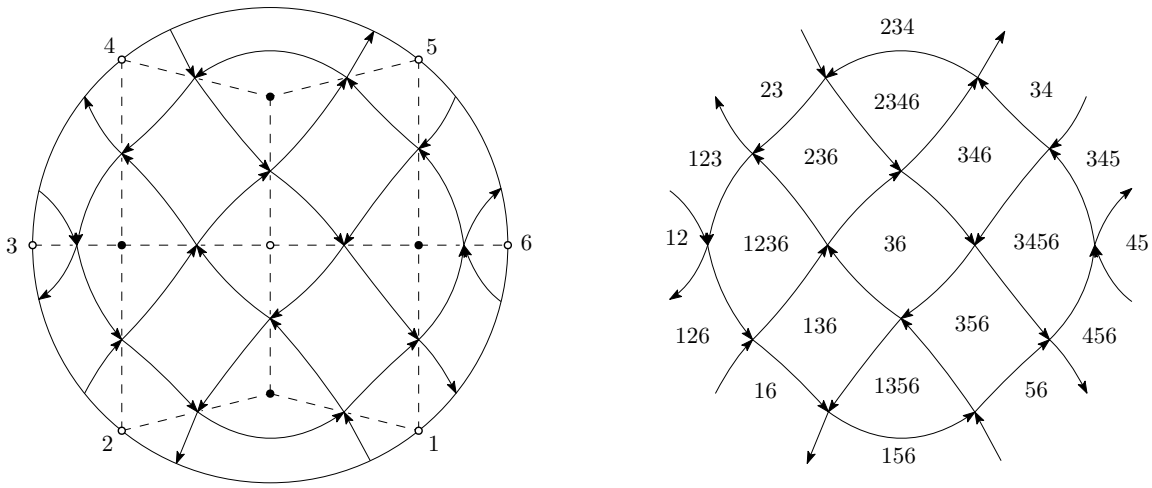

FIGURE 16. The alternating strand diagram for a plabic graph (left) and the associated labeling by sets of the faces and vertices of the graph (right)

4.4. **The reconstruction map.** In this subsection, we begin to prove the second part of Theorem 4.3. Specifically, we define a map Ψ which will turn out to be the inverse of the restriction of Φ to $\mathcal{C}_G^\circ$. As Ψ has the effect of reconstructing the entire configuration from just the boundary vectors, we term it the *reconstruction map*. We temporarily add an assumption on G that there is no isolated boundary vertex and no boundary vertex attached to vertex of degree 1. Since G is reduced this condition is equivalent to saying $\mathcal{M}$ has a basis containing j and one excluding j for each $j = 1, \ldots, n$. It follows that $j \in I_j$ and $j \notin I_{j+1}$.

It is convenient at this point to introduce an alternate representation of zigzag paths known as strands. A strand is obtained from a zigzag by taking each turn of the zigzag and replacing it with an arc connecting the midpoints of two edges involved. Based on the zigzag rules, the arc appears to go clockwise around a white vertex and counterclockwise around a black vertex. The *strand* is obtained by combining all arcs of a zigzag as well as small pieces at the beginning and end to connect it to the boundary of the disk. The strands together form an *alternating strand diagram*, one example of which is given in Figure 16. Note that strand number i begins slightly clockwise relative to boundary vertex i. An intersection of zigzags as defined previously translates to an intersection in the usual sense of strands.

Each region of an alternating strand diagram has boundary oriented clockwise, counterclockwise, or in an alternating manner, and the region corresponds respectively to a white vertex, black vertex, or face of G. Use the notations S_w, S_b, and S_F to denote the set of strands that the region in the strand diagram associated to w, b, or F lies to the left of. For F a face, this definition agrees with the previously given zigzag one. To avoid strands all together, one could define S_w and S_b in terms of zigzags as well, with the caveat that the black vertices of a zigzag are considered to be on its left while its white vertices are not.

Proposition 4.13. *Let F be a face of G, $b \in B$, and $w \in W$.*

- *$|S_F| = k$, $|S_w| = k-1$, and $|S_b| = k+1$.*
- *If b and w are on the boundary of F then $S_w \subseteq S_F \subseteq S_b$.*

Proof. It is standard that each S_F has size k. If w is a white vertex of F then there is a zigzag through w that enters and exits along the boundary of F and turns left at w. The corresponding strand divides the regions corresponding to F and w with the region corresponding to F on the left. Therefore S_w equals S_F less that one strand. In particular $S_w \subseteq S_F$ with $|S_w| = k-1$. A similar argument applies to black vertices. □

Fix $A \in T_G \subseteq \Pi_{\mathcal{M}}$ and in fact fix a particular matrix representative so that the columns $v_1, \ldots, v_n$ of A all live in V. Let $H_j \subseteq V$ denote the linear span of $\{v_i : i \in I_j \setminus \{j\}\}$. For each $w \in W$, define

$$L_w = \bigcap_{j \in S_w} H_j. \tag{4.8}$$

Recall our notation v_j' for column j of the right twist of A.

Lemma 4.14.

(1) Each H_j is a hyperplane with orthogonal complement spanned by v_j'
(2) The set $\{H_j : j \in S_F\}$ of k hyperplanes are in general position for each face F.
(3) Each L_w is a line.

Proof.

(1) Since $A \in T_G \subseteq \Pi^\circ_{\mathcal{M}}$ we know that $\Delta_{I_j}(A) \neq 0$ so the v_i with $i \in I_j$ is a basis of V. We know that $j \in I_j$ so H_j is a span of all but one of these vectors and is hence a hyperplane. The twist is defined in such a way that v'_j is nonzero and orthogonal to each v_i for $i \in I_j \setminus \{j\}$, so v'_j is the orthogonal complement of H_j.
(2) It is equivalent to say that the orthogonal vectors v'_j for $j \in S_F$ form a basis of V. By Theorem 4.2, this is true because $A \in T_G$.
(3) Fix w and let F be any face containing it. Then $S_w \subseteq S_F$ and $|S_w| = k-1$. So L_w is an intersection in $V = \mathbb{C}^k$ of $k-1$ hyperplanes in general position and is hence a line.

□

Proposition 4.15. *Let $b \in B$ and choose nonzero vectors $v_w \in L_w$ for each neighbor w of b. Then these v_w satisfy a unique linear relation up to scale, and this relation has all coefficients nonzero.*

Proof. Suppose b has degree d and let $j_1, \ldots, j_d$ be the numbers of the strands around b in counterclockwise order. For $i = 1, \ldots d$ there is a face F_i separated from b by strand j_i. There is an edge shared by F_{i-1} and F_i (indices modulo d) whose endpoints are b and some w_i. Then $w_1, \ldots, w_d$ are the neighbors of b and we have

- $S_{F_i} = S_b \setminus \{j_i\}$
- $S_{w_i} = S_b \setminus \{j_{i-1}, j_i\}$

Let $S = S_b \setminus \{j_1, \ldots, j_d\}$. Then for each i, $S \subseteq S_{w_i}$ so

$$v_{w_i} \in L_{w_i} \subseteq \cap_{a \in S} H_a.$$

Also, $S \subseteq S_{F_1}$ so the hyperplanes in this intersection are in general position. As $|S| = k+1-d$ we have that $\cap_{a \in S} H_a$ has dimension $d-1$. Therefore the d vectors v_{w_i} in this space must satisfy a relation.

Now suppose $c_1 v_{w_1} + \ldots + c_d v_{w_d} = 0$ is a non-trivial relation. Note that $j_1 \in S_{w_i}$ for all $i = 3, \ldots, d$, so $v_{w_i} \in H_{j_1}$ for these i. On the other hand, $v_{w_1} \notin H_{j_1}$ because otherwise we would have $v_{w_1} \in H_a$ for all $a \in S_{w_1} \cup \{j_1\} = S_{F_d}$ which would imply $v_{w_1} = 0$. A similar argument shows $v_{w_2} \notin H_{j_1}$. Therefore, we can apply a linear functional vanishing at H_{j_1} (e.g. the dot product with v'_{j_1}) to the above relation and precisely the first two terms survive. It follows that c_1 and c_2 are either both zero or both nonzero and have a prescribed ratio. The same is true by symmetry for each pair of consecutive coefficients. We cannot have all $c_i = 0$ so the c_i are all nonzero and are unique up to multiplication by a common factor. □

Proposition 4.16. *Let $A \in T_G$. Then there exists a unique configuration $(\mathbf{v}, \mathbf{R}) \in \mathcal{C}^\circ_G$ such that $\Phi(\mathbf{v}, \mathbf{R}) = A$ and $v_w \in L_w$ for all $w \in W$. This configuration has the property that the set of vectors neighboring each black vertex is a circuit.*

Proof. Let v_j equal column j of A. First we show $v_j \in L_j$ holds for these eventual boundary vectors. Consider the boundary face F of G containing the boundary segment between j and $j+1$. By [23, Proposition 4.3], S_F equals the set $\widetilde{I}_j$ in the so-called reverse Grassmann necklace of $\mathcal{M}$. The strand separating face F from white vertex j is in fact strand number j so $S_j = \widetilde{I}_j \setminus \{j\}$. To prove $v_j \in L_j$ it is equivalent to show that v_j is orthogonal to v'_i for each $i \in \widetilde{I}_j \setminus \{j\}$. This fact is part of the characterization of the inverse of the right twist (also known as the left twist) provided by Muller and Speyer [23].

To extend to a configuration with the desired properties, each internal v_w is determined up to scale since L_w is a line. Fixing a nonzero v_w for each w, we get by Proposition 4.15 that the associated relations R_b are also determined up to scale. In short, the whole configuration is determined up to gauge at internal vertices, giving us the uniqueness. That the relations have nonzero coefficients also gives us the circuit condition.

It remains to show that the vectors and relations $(\mathbf{v}, \mathbf{R})$ as above comprise a valid configuration on G. The only property not clear at this point is that the Kasteleyn matrix K is full rank. By Proposition 4.15 all coefficients K_{bw} with $\overline{bw} \in E$ are nonzero. By the general theory, there is a unique almost perfect matching of B with $W \setminus I_1$ (we describe a construction of this matching later on). Therefore the polynomial $\Delta_{W \setminus I_1}(K)$ of the coefficients is in fact a monomial and hence nonzero. □

We now have our definition of the reconstruction map $\Psi : T_G \to \mathcal{C}^\circ_G$, namely it maps A to the configuration given by Proposition 4.16. Clearly $\Phi \circ \Psi$ is the identity. In plainer terms we have existence of an extension of generic $A \in \Pi_{\mathcal{M}}$ to a full configuration. In principle, there could be other extensions with $v_w \notin L_w$ for some w, a possibility we rule out in the next subsection.

Example 4.17. Consider the plabic graph G in Figure 16. As previously discussed, G corresponds to the uniform matroid in $Gr_{3,6}$, and it follows that $I_j = \{j, j+1, j+2\}$ with indices modulo 6. Given $A = [v_1 \cdots v_6]$ then, $H_i = \langle v_{i+1}, v_{i+2} \rangle$. The unique internal white vertex w has $S_w = \{3, 6\}$, so

$$L_w = H_3 \cap H_6 = \langle v_4, v_5 \rangle \cap \langle v_1, v_2 \rangle.$$

Hence our general recipe reproduces the result argued in Example 1.6.

4.5. **Uniqueness.** If $A \in T_G$ we now know $\Phi(\Psi(A)) = A$. On the other hand, suppose $(\mathbf{v}, \mathbf{R}) \in \mathcal{C}_G^\circ$ and that $\Phi(\mathbf{v}, \mathbf{R}) = A$. We want to show $(\mathbf{v}, \mathbf{R}) = \Psi(A)$ in order to establish that preimages are unique. In light of Proposition 4.16, it is sufficient to show $v_w \in L_w$ for all internal white vertices w. The proof is in a sense recursive, utilizing a certain acyclic orientation on G.

A *perfect orientation* on G is an orientation with the property that each internal white vertex has a unique incoming edge and each (internal) black vertex has a unique outgoing edge. Given such an orientation, the set of edges oriented from black to white always give an almost perfect matching. We focus on one such orientation. Each edge of G is part of two zigzags that traverse it in opposite directions. Declare each edge to be oriented in the direction of its smaller numbered zigzag. We need a topological lemma before establishing the properties of this orientation.

Lemma 4.18. *Consider n simple curves between the boundary components of an annulus all having distinct endpoints from each other. Number the curves cyclically via the location of their endpoint on the inner boundary component. If no two consecutive curves intersect, then no two curves intersect at all.*

Proof. Number the curves 1 through n clockwise based on their endpoints on the inner circle. Curve i is simple so locally there is a notion of being clockwise or counterclockwise relative to i. If curve j intersects curve i then from its last intersection point with i it goes either clockwise or counterclockwise. Call the distance of the intersection either $j - i$ or $i - j$ in these respective cases, where in either case the distance is reduced modulo n to $\{1, \ldots, n-1\}$. Note distance 1 is not possible since consecutive curves do not intersect.

Suppose for the sake of contradiction curves intersect, and pick a pair i, j intersecting with minimal distance. Let's say j goes clockwise after its last intersection with i. The final segments of i and j separate the endpoints of curves $i+1, \ldots, j-1$ from the inner circle. Each such curve must either intersect i and go clockwise or intersect j and go counterclockwise. In either case we get a contradiction of the minimality of the distance $j - i$. □

Proposition 4.19. *The orientation on G defined above has the following properties:*

1. *It is a perfect orientation.*
2. *The corresponding matching uses precisely the boundary vertices $\{1, \ldots, n\} \setminus I_1$.*
3. *The matching uses exactly $m - 1$ edges from each internal $2m$-gon face.*
4. *The orientation is acyclic.*

Proof.

(1) Suppose zigzags $j_1, \ldots, j_d$ pass through a given black vertex b, and are arranged in clockwise order according to the edges along which they approach b. Passing to the strand diagram, segments of strands $j_1, \ldots, j_d$ form a topological circle around b with j_i and j_{i+1} intersecting at the point where j_i first reaches the circle. By reducedness, the strands do not intersect prior to that point. In particular, the segments of j_i and j_{i+1} from their beginnings to where they first reach the circle do not intersect. By Lemma 4.18 these n initial segments are all pairwise non-intersecting. As such, the start points are also in clockwise order. Applying a cyclic shift we can assume $j_1 < j_2 < \ldots < j_d$. Going back to zigzags shows that the edge through which j_d approaches b and j_1 departs it is the unique edge oriented away from b. A similar argument applies to white vertices.

(2) Each zigzag i starts at vertex i and ends at some $f(i)$. The function f is called the *trip permutation*. Let F be the boundary face of G between vertices n and 1. Then F is to the left of zigzag number i if and only if $f(i) < i$. By [23, Proposition 4.3], I_1 equals the set of target labels $f(i)$ of the strands for which this occurs, so $I_1 = \{f(i) : f(i) < i\}$.

Each boundary vertex j has degree one with zigzag j departing along its one edge and zigzag $f^{-1}(j)$ approaching. Unfolding definitions, j is part of the matching if and only if the edge is oriented towards j, if and only if $f^{-1}(j) < j$. By the above, this condition is equivalent to $j \notin I_1$.

(3) Let F be a face with $2m$ sides. Let $w_1, b_1, \ldots, w_m, b_m$ be the boundary vertices in clockwise order. Then there is a zigzag i_a with subpath b_a, w_a, b_{a-1} and a zigzag j_a with subpath w_a, b_a, w_{a+1}. By arguments similar to part 1 of this Proposition one can show that $i_1, \ldots, i_m$ are in cyclic order as are each triple i_{a+1}, j_a, i_a. Applying a cyclic shift we can assume $i_1 < \ldots < i_m$.

Consider black vertex b_a for $1 \leq a < m$. The zigzags i_{a+1}, j_a, i_a all include b_a and are consecutive in the clockwise order on such paths. Since $i_{a+1} > i_a$, we have that the cyclic order on i_{a+1}, j_a, i_a wraps around on one or the other side of j_a. By the proof of part 1, the edge of the matching through b_a is part of j_a and is hence on the boundary of F. On the other hand, consider b_m which lies on each of i_1, j_m, i_m. Since $i_1 < i_m$ the cyclic order implies $i_1 < j_m < i_m$. As such, the edge of the matching containing b_m is not part of j_m, hence not part of F.

Each edge of the matching using an edge of F uses exactly one black vertex from the boundary of F. We have shown there are $m - 1$ such black vertices, so there are $m - 1$ such edges as desired.

(4) Suppose for the sake of contradiction that G had a cycle. Half of the edges of the cycle, namely those going from black to white, appear in the matching. Another matching is obtained by taking out all of

these edges and including the other half of the edges of the cycle. The result is another almost perfect matching using the same boundary vertices.

By Muller and Speyer [23], the set of almost perfect matchings using a fixed set of boundary vertices is a distributive lattice. Moreover, they show that the cover relations in this partial order correspond to flips in internal faces of which one half the edges are used in the first matching and the other half in the second. By the previous part, the matching we have constructed does not use half the edges of any internal faces. Therefore it is alone among those avoiding the set I_1. The second matching constructed above gives a contradiction.

□

Let π be the almost perfect matching defined above. More directly, π is the set of edges of G through which the smaller numbered zigzag goes from the black endpoint to the white endpoint. This matching can easily be seen to be among the extremal matchings defined by Muller and Speyer [23] in terms of downstream wedges. From this point of view the properties listed above can be attributed to them.

Corollary 4.20. *Suppose* $(\mathbf{v}, \mathbf{R}) \in \mathcal{C}_G$ *and that* $\{v_j : j \in I_1\}$ *is a basis for* V*. Then* $K_{bw} \neq 0$ *for each edge* $\overline{bw}$ *in the matching* π*.*

Proof. By Corollary 4.6, we know $\Delta_{W \setminus I_1}(K) \neq 0$. By the proof of Proposition 4.19, π is the unique matching of $W \setminus I_1$ with B. As such the determinant equals (up to sign) the product of the weights K_{bw} of the edges of the matching. Therefore each such weight must be nonzero. □

Proposition 4.21. *Suppose* $(\mathbf{v}, \mathbf{R}) \in \mathcal{C}_G$ *and that* $\{v_j : j \in I_1\}$ *is a basis for* V*. Recall* H_1 *is the span of the vectors* v_j *for* $j \in I_1 \setminus \{1\}$*. If* w *is a white vertex and there is no path from boundary vertex* 1 *to* w *then* $v_w \in H_1$*.*

Proof. Let b be the black vertex such that $\overline{bw}$ is the unique edge incident to and directed towards w. By Corollary 4.20, $K_{bw} \neq 0$. As $\sum_{w'} K_{bw'} v_{w'} = 0$, we have that v_w lies in the span of the $v_{w'}$ for w' the other neighbors of b. Note that all edges $\overline{w'b}$ with $w' \neq w$ are oriented towards b so there is a length 2 path from each w' to w. We can apply the same argument recursively to each w'. Since the orientation is acyclic the end result is that v_w lies in the span of those v_j with j a source (i.e. $j \in I_1$) for which there exists a path from j to w. By assumption there is no such path from 1 so $v_w \in H_1$ as desired. □

Lemma 4.22. *Let* w *be any white vertex, internal or boundary. If* w *lies strictly left of the zigzag starting at* 1 *then there is no oriented path from* 1 *to* w*.*

Proof. First note that every edge of zigzag 1 is oriented in the direction of zigzag 1. In other words, zigzag 1 is an oriented path. We claim there is no oriented edge starting weakly right of the zigzag and ending strictly left of the zigzag. The proof is case by case depending on the start vertex of the edge. If the edge starts strictly right of the zigzag then it must end weakly right of the zigzag (otherwise it would cross it and break planarity). If the edge starts on the zigzag at a black vertex b then it must be the unique edge oriented away from b. We know that this edge is part of the zigzag so it ends on the zigzag. Lastly, suppose our given edge starts at a white vertex w on the zigzag. The zigzag locally looks like b, w, b' where b' is reached by turning maximally left at w. As such, all the edges incident to w lie weakly to the right of the zigzag. □

Combining Proposition 4.21 and Lemma 4.22, we have that v_w lies on H_1 if w is strictly left of the zigzag starting at 1. The analogous result holds for each start vertex. We are now ready to prove the uniqueness result.

Proposition 4.23. *Let* $(\mathbf{v}, \mathbf{R}) \in \mathcal{C}_G^\circ$ *and suppose* $A = \Phi(\mathbf{v}) \in T_G$*. Then* $(\mathbf{v}, \mathbf{R}) = \Psi(A)$*.*

Proof. Suppose $A = \Phi(\mathbf{v}) \in T_G$. Then A is in the open positroid variety so the set of columns of A corresponding to I_j is a basis of V for all j. Fix $w \in W$ internal. For each $j \in S_w$ we have the assumptions of Proposition 4.21 (with 1 replace by j), so $v_w \in H_j$. Therefore $v_w \in L_w$. By Proposition 4.16, $(\mathbf{v}, \mathbf{R})$ is in fact the same as $\Psi(A)$. □

By Proposition 4.9, the image of Φ restricted to $\mathcal{C}_G^\circ$ equals the image of the boundary measurement map, which by definition equals T_G. As such the condition $\Phi(\mathbf{v}) \in T_G$ in Proposition 4.23 is redundant. In short $\Psi \circ \Phi$ is defined on all of $\mathcal{C}_G^\circ$ and in fact equals the identity on that set. This completes the proof of Part 2 of Theorem 4.3. It follows that $\mathcal{C}_G^\circ$ equals the image of Ψ, which has an unexpected consequence.

Proposition 4.24. *Let* $(\mathbf{v}, \mathbf{R}) \in \mathcal{C}_G$*. Then* $(\mathbf{v}, \mathbf{R}) \in \mathcal{C}_G^\circ$ *if and only if the* v_w *neighboring each* $b \in B$ *are a circuit.*

Proof. Recall $\mathcal{C}_G^\circ$ was defined by the condition that each coefficient K_{bw} for $\overline{bw} \in E$ is nonzero. A relation among vectors must have nonzero coefficients if the vectors form a circuit, but the converse is not in general true. However, something about the global structure of $\mathcal{C}_G^\circ$ ensures that the vectors in each relation form a

circuit. Indeed if $(\mathbf{v},\mathbf{R}) \in \mathcal{C}_G^\circ$ then $(\mathbf{v},\mathbf{R})$ is in the image of Ψ and the desired result follows from Proposition 4.16. □

Proof of Theorem 4.3. All that remains is Part 3. We already know if $(\mathbf{v},\mathbf{R}) \in \mathcal{C}_G^\circ$ then $\Phi(\mathbf{v},\mathbf{R}) \in T_G$. On the other hand, suppose $A \in T_G$ and that $\Phi(\mathbf{v},\mathbf{R}) = A$. We know $\Delta_{\{1,\dots,n\}\setminus I_1}(A) \neq 0$ so by Corollary 4.20 each $K_{bw} \neq 0$ for $\overline{bw}$ in the matching π. By definition of π, this in particular is true on any edge which zigzag number 1 traverses from black to white. For a general edge, it is traversed from black to white by some zigzag j and we get the same result by taking the matching defined the same way relative to the order $j < \ldots < n < 1 < \ldots < j-1$ on zigzags. All coefficients are nonzero so $(\mathbf{v},\mathbf{R}) \in \mathcal{C}_G^\circ$.

We have assumed at various points that G has no isolated boundary vertex and no boundary vertex attached to a degree 1 vertex. We briefly describe modifications needed to handle these cases. First suppose j is an isolated boundary vertex of G. One can consider the strand of j to be a simple arc disjoint from G starting at a point clockwise from j and ending at a point counterclockwise from j. All definitions and proofs go through except a simple argument needs to be added to part 2 of Proposition 4.19.

Now suppose j is attached to a degree 1 vertex b. The strand for j loops around b and self-intersects before returning to the boundary, causing a few problems including in the definition of the reconstruction map. It is consistent to have all other $S_F, S_w, S_{b'}$ omit j, but there is no clear definition for S_j and S_b. That said, j is part of every almost perfect matching so it is part of no basis of $\mathcal{M}$. Hence any $A \in \Pi_{\mathcal{M}}$ has jth column $v_j = 0$. As such, we can define $\Psi(A)$ to have $v_j = 0$ and $R_b = 1v_j$, and define all other vectors and relations in a manner independent of the index j. Elsewhere, the orientation we define is ambiguous regarding how to orient the edge $\overline{jb}$. In fact it must be oriented towards j to get a perfect orientation, and this choice does not cause any other issues. □

4.6. **Geometric interpretation of edge weights.** We now shift focus back to the boundary measurement map and describe a geometric interpretation of the edge weights in terms of vector configurations. To this end, it is more convenient to use Postnikov's original formulation of the boundary measurement map in terms of path families [26], which we now review.

Postnikov's construction depends on a choice of a perfect orientation on G. We only consider the special case of the acyclic orientation from before where each edge of G is oriented in the direction of its smaller numbered zigzag. Assume G is given positive real edge weights and define the weight of a directed path to be the product of the weights of its edges traversed from white to black divided by the product of weights of edges traversed from black to white. Recall the set of sources is I_1. For $i \in I_1$ and $j \in \{1,\dots,n\}$ let M_{ij} be the sum of the weights of all oriented paths from i to j. Pick a basis $\{\widetilde{v}_i : i \in I_1\}$ of $\mathbb{R}^k$ and for general j let $\widetilde{v}_j = \sum_i M_{ij}\widetilde{v}_i$. Then the output of the boundary measurement map is the point $A = [v_1 \cdots v_n] \in Gr_{k,n}$ where $v_j = \sigma_j \widetilde{v}_j$ and the σ_j are certain signs. Specifically,

$$\sigma_j = (-1)^{|I_1 \cap \{1,2,\dots,j\}|-1}.$$

Remark 4.25. It is common to take the $\widetilde{v}_i$ with $i \in I_1$ to be the ordered standard basis. Assuming this convention, Postnikov does take the M_{ij} with certain signs as the entries of A, but our signs are different from his. We get a different representative matrix A but the same point in the Grassmannian (we omit the proof of this fact). Note our formula for σ_j only works for this specific perfect orientation.

There is an efficient recursive method to calculate the boundary measurement map. Indeed, for any source i and white vertex w define M_{iw} to be the sum of the weights of paths from i to w. Fix any nonsource w and let b be its unique neighbor such that $e = \overline{bw}$ is directed towards w. All other neighbors w' of b are such that $\overline{bw'}$ is directed towards b. So a path from i to w is given by a path from i to some such w' followed by the length two path w' to b to w. Hence

$$M_{iw} = \frac{1}{\mathrm{wt}(e)} \sum_{w'} \mathrm{wt}(\overline{bw'}) M_{iw'}.$$

As the orientation is acyclic, this gives a well-defined recursion starting from $M_{iw} = \delta_{iw}$ for $w \in I_1$. We can just as well work on the level of vectors defining $\widetilde{v}_w$ recursively by

$$\widetilde{v}_w = \frac{1}{\mathrm{wt}(e)} \sum_{w'} \mathrm{wt}(\overline{bw'}) \widetilde{v}_{w'}. \tag{4.9}$$

As b varies, the relations (4.9) show that the vectors $\widetilde{v}_w$ form a configuration $\widetilde{\mathbf{v}} \in \mathcal{C}_G^\circ$. It has the added feature that each vector is a positive combination of the vectors 2 steps upstream from it, and in particular all vectors are in the positive orthant relative to the basis $\{\widetilde{v}_i : i \in I_1\}$. More can be said. Using acyclicity again, we can apply gauges at internal vertices so that the sum of the weights of incoming edges to each internal vertex equals 1. In the notation above, e is the unique incoming edge to w so if w is internal then $\mathrm{wt}(e) = 1$ and the coefficients in (4.9) sum to 1. So $\widetilde{v}_w$ is a convex combination of the $\widetilde{v}'_w$.

Example 4.26. Figure 17 shows a plabic graph G for $Gr_{3,6}$. Assume gauge has been applied so that the weights of edges entering each internal vertex sum to 1. As $I_1 = \{1,2,3\}$ only $\sigma_2 = -1$ so we can suppress the $\sim$'s

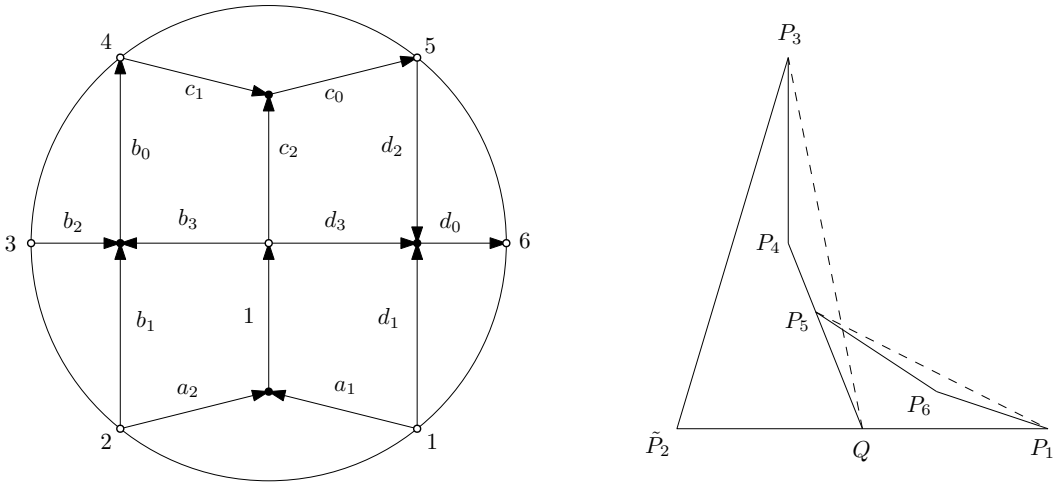

FIGURE 17. A plabic graph with an acyclic perfect orientation (left) and a configuration that results from the associated sequence of convex combinations (right)

in the $\widetilde{v}_j$ except for $j = 2$. Let u be the vector at the interior white vertex. Let $v_1, \widetilde{v}_2, v_3$ be any basis of $\mathbb{R}^3$. Following the arrows we construct

$$\begin{aligned} u &= a_1 v_1 + a_2 \widetilde{v}_2 \\ v_4 &= \frac{1}{b_0}(b_1 \widetilde{v}_2 + b_2 v_3 + b_3 u) \\ v_5 &= \frac{1}{c_0}(c_1 v_4 + c_2 u) \\ v_6 &= \frac{1}{d_0}(d_1 v_1 + d_2 v_5 + d_3 u) \end{aligned}$$

The output of the boundary measurement map is $[v_1 v_2 \cdots v_6]$ where $v_2 = -\widetilde{v}_2$.

If we allow gauge at boundary vertices, which corresponds to modding out by the torus action on the Grassmaian, we can additionally arrange $b_0 = c_0 = d_0 = 1$. Each vector is constructed as a convex combination of its predecessors with coefficients given by the edge weights. It is easier to draw the picture in the projective plane replacing the vectors $v_1, \widetilde{v}_2, \ldots v_6, u$ with points $P_1, \widetilde{P}_2, \ldots, P_6, Q$ (see the right of Figure 17). The points are constructed in the same way: start with $P_1, \widetilde{P}_2, P_3$, pick Q on segment $\overline{P_1 \widetilde{P}_2}$, pick P_4 in triangle $\triangle \widetilde{P}_2 P_3 Q$, pick P_5 on segment $\overline{P_4 Q}$, and pick P_6 in $\triangle P_1 P_5 Q$.

Proposition 4.27. *Let $A = [v_1 \cdots v_n] \in \Pi_{\mathcal{M},>0}$ and consider the problem of recovering the edge weights on G of its preimage under the boundary measurement map. To this end, construct the following data:*

- *$\widetilde{A} = [\widetilde{v}_1 \cdots \widetilde{v}_n] \in \Pi^\circ_{\mathcal{M}}$ where $\widetilde{v}_j = \sigma_j v_j$*
- *$\widetilde{\mathbf{v}} = \Psi(A)$ with gauge chosen so that each $\widetilde{v}_w$ for w internal is a convex combination of the vectors 2 steps upstream from it.*

Fix b and adopt notation as in (4.9). If w is internal then $\mathrm{wt}(e) = 1$ and the $\mathrm{wt}(\overline{bw'})$ are the barycentric coordinates of v_w relative to the v'_w. If w is on the boundary then $\mathrm{wt}(e)$ is the number λ so that λv_w is a convex combination of the v'_w and the other edge weights are the barycentric coordinates of λv_w.

The proof is immediate as we are just undoing the boundary measurement map as described in this section. The vectors $\widetilde{v}_w$ constructed by Ψ must agree with the ones built recursively by the boundary measurement map thanks to the uniqueness result Proposition 4.23. Since Ψ is defined via intersection of hyperplanes we get a geometric meaning for the edge weights. Note that the problem of recovering the edge weights was solved for Le-diagrams by Talaska [30] and in general by Muller and Speyer [23].

Example 4.28. Continue with G as in Figure 17 and Example 4.26. Let $A = [v_1 \cdots v_6] \in Gr_{3,6}$ with all minors positive. Let $\widetilde{v}_2 = -v_2$. As discussed in previous examples, the internal vector u satisfies

$$u \in \langle v_1, v_2 \rangle \cap \langle v_4, v_5 \rangle.$$

We know all vectors lie in the cone spanned by $v_1, \widetilde{v}_2, v_3$. Projecting to the affine plane spanned by the endpoints of these vectors produces a picture as in the right of Figure 17. As such, a_1, a_2 are the barycentric coordinates of $Q = \langle P_1, \widetilde{P}_2 \rangle \cap \langle P_4, P_5 \rangle$ relative to $P_1, \widetilde{P}_2$.

Alternately, a direct formula for a_1, a_2 can be derived as follows. A candidate for u is

$$|v_2 v_4 v_5| v_1 - |v_1 v_4 v_5| v_2 = -|v_1 v_2 v_5| v_4 + |v_1 v_2 v_4| v_5.$$

We want a convex combination $a_1 v_1 + a_2 \widetilde{v}_2 = a_1 v_1 - a_2 v_2$ so we scale down to get

$$a_1 = \frac{|v_2 v_4 v_5|}{|v_1 v_4 v_5| + |v_2 v_4 v_5|}, \qquad a_2 = \frac{|v_1 v_4 v_5|}{|v_1 v_4 v_5| + |v_2 v_4 v_5|}.$$

Remark 4.29. The shape of the relation (4.9) suggests possible Kasteleyn signs for G. Specifically, let π be the almost perfect matching consisting of the set of edges directed from black to white. It is tempting to define the signs of edges of π to be negative and all others positive. Part 3 of Proposition 4.19 verifies that the result does in fact satisfy the Kasteleyn condition at each internal face, but the boundary faces do not end up working out. This issue can be resolved by taking the signs just described and applying gauge by σ_j at each boundary vertex j.

Remark 4.30. The matrix $\widetilde{A}$ with certain columns negated has some advantages over the traditional output A of the boundary measurement map. For instance, the usual picture for a totally positive point $A \in Gr_{3,n}$ is to project the columns and obtain the vertices of a convex n-gon P. An intersection point like $\langle P_1, P_2\rangle \cap \langle P_4, P_5\rangle$ could lie on either side of the polygon or even at infinity. Now consider $\widetilde{A}$. In this case $\sigma_2 = -1$ and all other $\sigma_j = 1$. The picture in the plane is that $P_1, \widetilde{P}_2, P_3$ form a triangle and $P_3, P_4, \ldots, P_n, P_1$ form a convex polygonal curve in its interior (see Figure 17). The hyperplanes spanned by pairs of consecutive points all intersect in predictable regions.

5. Structure of the space $\mathcal{C}_G$

Let G be a plabic graph with all of the conventions and notation of Section 4. We have defined $\mathcal{C}_G$ as the set of vector-relation configurations on G modulo gauge transformations at internal vertices and the action of $GL_k(\mathbb{C})$. In this section we consider the algebraic-geometric structure both of $\mathcal{C}_G$ and of the function Φ which by Theorem 4.3 maps it to the positroid variety Π_G.

First, consider a configuration $\mathbf{v} \in \mathcal{C}_G$. We will describe explicitly a bijection between a neighborhood of $\mathbf{v}$ and an open subset of an affine variety. Since the boundary vectors $v_1, \ldots, v_n$ span V, there must be a basis $\{v_j : j \in I\}$ among them. Acting by GL_k we can arrange for this to equal the standard basis in order. Next, each internal vector v_w is nonzero so we can pick one of its nonzero entries and apply a gauge so that the entry equals 1. Finally, by Lemma 4.5 we know that

$$\Delta_{W \setminus I}(K) \neq 0.$$

It follows that there is an almost perfect matching of B with $W \setminus I$ with all K_{bw} along the matching nonzero. Apply gauge at the black vertices to scale all these K_{bw} to 1.

We have exhausted the allowable operations, so the collection of remaining variables give a well-defined map to affine space. Specifically, the coordinates are the entries of the boundary vectors v_j with $j \notin I$, each entry of each internal vector v_w except the one scaled to 1, and all the K_{bw} for edges $\overline{bw}$ not in the matching. The map to affine space is injective and it is easy to describe the image. For each $b \in B$ the vector relation $\sum_w K_{bw} v_w = 0$ amounts to k quadratic relations in the variables. The only other condition is that the matrix K has full rank. Restricting the chart a bit, we can replace this with the single inequality $\Delta_{W \setminus I}(K) \neq 0$ which as already mentioned holds for $\mathbf{v}$.

Example 5.1. The graph G in Figure 18 is one of the standard plabic graphs for the open cell in $Gr_{2,4}$. Suppose a point $\mathbf{v} \in \mathcal{C}_G$ is given such that $\{v_1, v_3\}$ is a basis of $\mathbb{C}^2$, v_2 appears non-trivially in the relation on v_2, v_3, v_4, and v_4 appears non-trivially in the relation on v_1, v_2, v_4. The normalization described above produces the configuration in the figure where the edge variables indicate the coefficients of the relations. From the vector relations $v_2 + a v_3 + b v_4 = 0$ and $c v_1 + d v_2 + v_4 = 0$ we obtain the system

$$\begin{aligned} x_2 + b x_4 &= 0 \\ y_2 + a + b y_4 &= 0 \\ c + d x_2 + x_4 &= 0 \\ d y_2 + y_4 &= 0 \end{aligned}$$

The Kasteleyn matrix is

$$\begin{bmatrix} 0 & 1 & a & b \\ c & d & 0 & 1 \end{bmatrix}.$$

Taking the columns not in our basis we want $\Delta_{24}(K) = 1 - bd \neq 0$. The image of the chart is defined in affine space $\mathbb{C}^8$ by the four equations above and this one inequality.

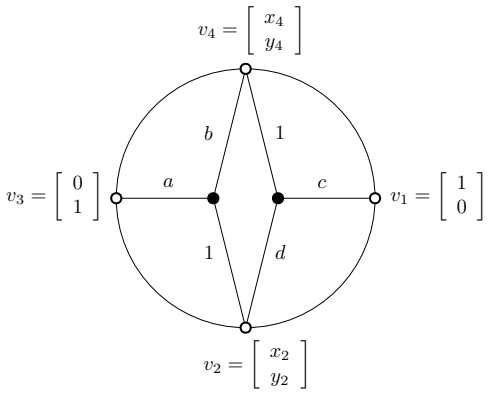

FIGURE 18. One chart on $\mathcal{C}_G$ with G a plabic graph corresponding to $Gr_{2,4}$.

In fact, a more efficient chart is obtained by taking just a, b, c, d as coordinates. The other variables can be reconstructed as

$$x_2 = \frac{bc}{1-bd} \qquad x_4 = -\frac{c}{1-bd}$$
$$y_2 = -\frac{a}{1-bd} \qquad y_4 = \frac{ad}{1-bd}$$

and as before we assume $1 - bd \neq 0$. The image of the chart is an open subset of $\mathbb{C}^4$, so in particular it is smooth.

We now state the main result for this section.

Theorem 5.2. *The space $\mathcal{C}_G$ of configurations on any reduced plabic graph G is smooth.*

The images of the charts defined above have lots of defining equations which make analysis somewhat difficult. Generalizing Example 5.1, we introduce more intricate charts which have the advantage of landing in open subsets of affine space. The atlas that results is indexed by certain subgraphs of G.

Say a subgraph $F = (B \cup W, E')$ of $G = (B \cup W, E)$ is a *system* in G if

- F is a forest,
- each component of F includes exactly one boundary vertex of G, and
- each component of F either contains exactly one edge or has the property that all of its black vertices have degree 2.

We choose the name because F has the appearance of a system of rivers connecting various points on an island to the surrounding ocean.

Proposition 5.3. *Let $F = (B \cup W, E')$ be a system in G. Suppose a configuration $\mathbf{v} \in \mathcal{C}_G$ has the property that $K_{bw} \neq 0$ for all $\overline{bw} \in E'$. Then there is a unique representative of the gauge class of $\mathbf{v}$ so that $K_{bw} = 1$ for all $\overline{bw} \in E'$.*

Proof. There is a unique simple path in F from each internal vertex to the boundary. Define a partial order on the set of internal vertices via $a \preceq a'$ if a lies on the path from a' to the boundary. Go through the internal vertices in a manner consistent with this order. At each a apply gauge to set equal to 1 the coefficient at the first edge on the path from a to the boundary. Each K_{bw} will be set to 1 after the gauge at whichever of b or w is larger in the order, and it will remain unchanged thereafter. It is easy to see that all choices for this gauge were forced, so the outcome is unique. □

We now have a rational map $\varphi_F : \mathcal{C}_G \to \mathbb{C}^{|E \setminus E'|}$. The map inputs a configuration $\mathbf{v}$, performs the gauge described in Proposition 5.3, and outputs the remaining coefficients K_{bw} for $\overline{bw} \notin E'$. On the other hand, given a point in $c \in \mathbb{C}^{|E \setminus E'|}$ we can construct a matrix K by setting

$$K_{bw} = \begin{cases} 1, & \text{if } \overline{bw} \in E' \\ c_{bw}, & \text{if } \overline{bw} \in E \setminus E' \\ 0, & \text{otherwise} \end{cases}$$

As explained in the paragraph following Lemma 4.4, an element of $\mathcal{C}_G$ is determined by its Kasteleyn matrix so we can recover $\mathbf{v}$. Therefore φ_F is injective.

Proposition 5.4. *The image of φ_F is dense in $\mathbb{C}^{|E \setminus E'|}$.*

Proof. Given $c \in \mathbb{C}^{|E \setminus E'|}$ we can construct K as above and then use Lemma 4.4 to build a configuration $\mathbf{v}$ in $\mathbb{C}^N/\mathrm{row}(K)$. The only difficulty would be if $\mathbf{v}$ violated one of the conditions in the definition of $\mathcal{C}_G$, each of which is easily seen to be stated in terms of an inequality. Specifically we need

- K is full rank, i.e. some $\Delta_S(K) \neq 0$,
- the boundary vectors $v_1, \ldots, v_n$ span V (equivalently some subset of them is a basis), i.e. some $\Delta_{W \setminus J}(K) \neq 0$ with $J \subseteq \{1, \ldots, n\}$, and
- for all w internal v_w is nonzero (equivalently v_w is part of a basis with other vectors of $\mathbf{v}$), i.e. some $\Delta_S(K) \neq 0$ with $w \notin S$.

□

Everything so far has only used the first two conditions of a system, namely that it is a forest with exactly one boundary vertex per component. The next result, which identifies the origin of each chart, clarifies the significance of the third condition.

Proposition 5.5. *The origin $0 \in \mathbb{C}^{|E \setminus E'|}$ is in the image of φ_F. It represents a configuration where a certain k boundary vectors form a basis, the other boundary vectors are 0, and each internal vector is proportional to the boundary vector in the same component.*

Proof. First note each single edge component of F is balanced as it has 1 black and 1 white vertex. Meanwhile, every other component has exactly one more white vertex than black. Indeed the number of edges of the component is one less than the number of vertices (since it is a tree) and twice the number of black vertices (since each black vertex has degree 2). So the number of non-single edge components must equal $N - M = k$. Let J be the set of boundary vertices of these components.

It is convenient to consider F to be a non-reduced plabic graph. Let F_j be the component of F containing boundary vertex j. Fix $j \in J$ and w a white vertex of F_j. Then there is a unique matching in F_j of all vertices other than j: simply match each back vertex with the one of its two neighbors not in the direction of w. Every matching of all of B in F consists of combining one matching as above for all $j \in J$ along with all of the edges of the single edge components. Taking the boundary vertex of each component we have a unique almost perfect matching π of B with $W \setminus J$. For $w \in W$ internal, let F_j be the component containing it. We can modify π along F_j so that it includes j instead of w. The result is a matching π_w of B with $W \setminus S$ where $S = (J \setminus \{j\}) \cup \{w\}$.

Consider the point $0 \in \mathbb{C}^{|E \setminus E'|}$ which corresponds to the zero-one matrix K with $K_{bw} = 1$ precisely for $\overline{bw} \in E'$. The matchings π and π_w witness the conditions from Proposition 5.4 for this point to be in the image of φ_F. Consider the associated configuration $\mathbf{v}$. If $j \in \{1, \ldots, n\} \setminus J$ then j is part of a single edge component. The black vertex of this component gives the relation $v_j = 0$. It follows that the v_j for $j \in J$ must be a basis. Each internal black vertex gives a relation $u + u' = 0$ among its two neighbor vectors in F. By induction, all vectors in a given component of F are proportional to each other. □

Proof of Theorem 5.2. Let $\mathbf{v} \in \mathcal{C}_G$. We will construct a system F so that φ_F is defined at $\mathbf{v}$. As such we get an identification of a neighborhood of $\mathbf{v}$ with an open set in affine space proving that $\mathcal{C}_G$ is smooth at $\mathbf{v}$.

Let $J \subseteq \{1, \ldots, n\}$ be such that $\{v_j : j \in J\}$ is a basis of V. Then there is an almost perfect matching π of B with $W \setminus J$ such that $K_{bw} \neq 0$ for all $\overline{bw} \in \pi$. We will start from the graph $F = (B \cup W, \pi)$ and add edges one at a time maintaining the properties

- F is a forest
- each component of F includes at most one boundary vertex
- each non-single edge component of F is connected to the boundary and has all its black vertices degree 2
- each edge of F has a nonzero coefficient K_{bw}

until all vertices are connected to the boundary. The result will be a system F with φ_F defined at $\mathbf{v}$.

Suppose we are at a stage where not all vertices of F are connected to the boundary. There are never isolated black vertices, so there must be a white vertex w not connected to the boundary. Since $v_w \neq 0$, it can be swapped into $\{v_j : j \in J\}$ so that the result is still a basis. Suppose $j \in J$ is such that v_j is the vector that got swapped out. Then there is a matching π' of B that avoids the white vertices $(J \setminus \{j\}) \cup \{w\}$ and that has all edge variables nonzero. The disjoint union of π and π' has degree ≤ 2 at each vertex and degree 1 at only w and j. As such it contains a path from w to j which we consider oriented in that direction. Let e be the first edge of this path whose target is connected to the boundary in F. Then the source of e is not connected to the boundary in F, so e is not in F and in particular e is not in π. Therefore e is in π' from which it follows that e goes from black to white. Adding e to F merges a single edge internal component to a boundary-connected component along a black vertex of the former. All the properties listed above are easily verified.

As it is always possible to find an additional edge, the above process does not terminate until all vertices are connected to a boundary. It follows at that point that F is a system as desired. □

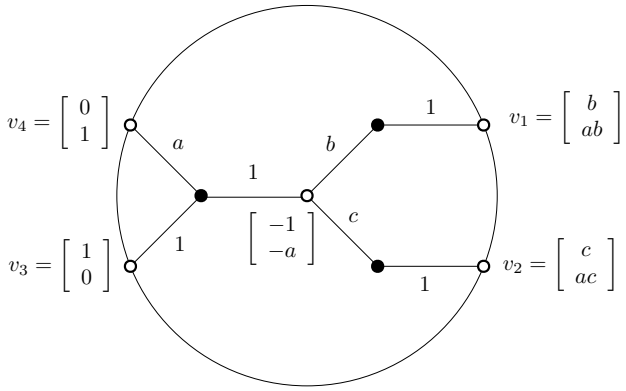

FIGURE 19. An example of a coordinate chart on $\mathcal{C}_G$ coming from a system in G.

Combining with results from the previous section, we have that $\Phi : \mathcal{C}_G \to \Pi_{\mathcal{M}}$ maps a smooth variety to the positroid variety and restricts to an isomorphism from $\mathcal{C}_G^\circ$ to T_G. Although Φ is not surjective, it can resolve certain singularities of $\Pi_{\mathcal{M}}$ as the next example illustrates.

Example 5.6. Consider the plabic graph G in Figure 19. The four edges of a system F have been labeled with 1's and the other three edges assigned coordinates a, b, c. We have that $J = \{3, 4\}$ are the boundary vertices of the non-single edge components of F so we can take v_3, v_4 as a basis. It is then possible to determine the vectors at the other three white vertices. In these coordinates, the map Φ takes the form

$$(a, b, c) \in \mathbb{C}^3 \mapsto \begin{bmatrix} b & c & 1 & 0 \\ ab & ac & 0 & 1 \end{bmatrix} \in \Pi_{\mathcal{M}} \subseteq Gr_{2,4}.$$

The target $\Pi_{\mathcal{M}}$ of Φ in this case is a Schubert variety defined in $Gr_{2,4}$ by the single equation $\Delta_{12} = 0$. This variety has a unique singular point given in matrix form by

$$A_{\text{sing}} = \begin{bmatrix} 0 & 0 & 1 & 0 \\ 0 & 0 & 0 & 1 \end{bmatrix}.$$

If $A = [v_1 v_2 v_3 v_4] \neq A_{\text{sing}}$ then v_1, v_2 are dependent but not both zero, so they span a line. The rightmost two black vertices in the plabic graph force the vector u at the internal white vertex to lie on this line. One can check, then, that the three relations of a configuration are always determined up to scale. So A has a unique preimage in $\mathcal{C}_G$.

On the other hand, let $A = A_{\text{sing}}$. Then $v_1 = v_2 = 0$ and the internal vector $u \in \mathbb{C}^2$ becomes arbitrary. As we only consider u up to scale, we have a $\mathbb{P}^1$ worth of preimages. This is the standard picture of the blowup of a variety at a point. Alternately, we can analyze the situation in coordinates. Restricting to the above chart we get a set $\{(a, 0, 0) : a \in \mathbb{C}\}$ of preimages of A. The last preimage, corresponding to the point at infinity in $\mathbb{P}^1$, lies outside the chart.

6. The resistor and Ising subvarieties

Goncharov and Kenyon [13] give a recipe to go from a resistor network given by an arbitrary weighted graph to a line bundle with connection on an associated bipartite graph. The resulting face weights satisfy some simple relations. There is an analogous recipe starting from the Ising model on a graph [6, 8, 15]. In this section we describe the vector-relation configurations that arise this way, focusing on the case when the initial network is on a triangular grid.

A resistor network is a plane graph $G = (V, E)$ with each edge assigned a positive real weight interpreted as its conductance (i.e. reciprocal of resistance). Suppose we draw the dual graph $G^* = (V^*, E^*)$ superimposed over a drawing of G. The resulting picture can be interpreted as a bipartite graph Γ whose white vertex set is $V \cup V^*$ and whose black vertices are the intersection points of dual edge pairs $e \in E, e^* \in E^*$. Each edge of both G and G^* is subdivided in two, and all of the resulting half edges together comprise the edge set of Γ. Assign each half of an edge in E the same weight as the original edge, and assign each half of an edge in E^* a weight of 1. Figure 20 illustrates the construction starting from a portion of the triangular grid graph G.

Let $G = (V, E)$ be the graph given by an infinite triangular grid and let Γ be the associated bipartite graph. Comparing Figures 10 and 20, we see that vector relation configurations on Γ give three generations of a Q-net. By Proposition 2.1, we can introduce signs to the weights coming from G to get such a configuration.

Proposition 6.1. *Suppose $(Q_{i,j,k})$ is a Q-net constructed from a resistor network as above. Then it is in fact a discrete Koenigs net. In particular the points $Q_{i,j,k}$, $Q_{i+1,j+1,k}$, $Q_{i+1,j,k+1}$, and $Q_{i,j+1,k+1}$ are coplanar for all $i, j, k \in \mathbb{Z}$.*

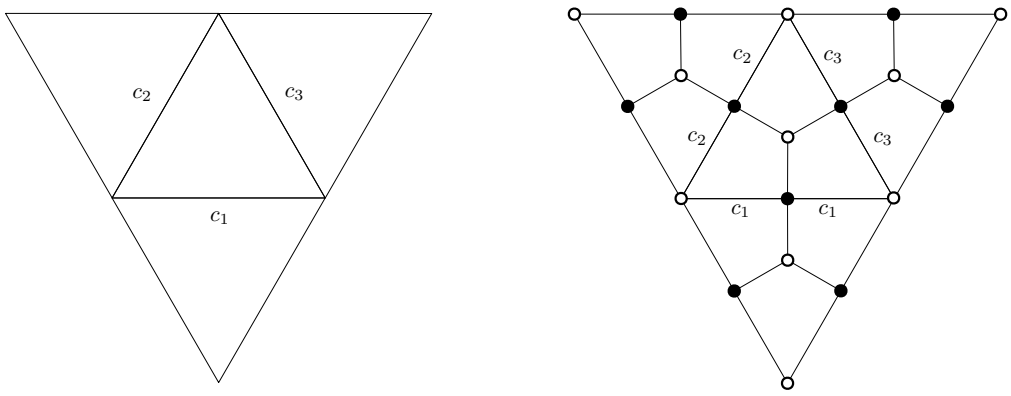

FIGURE 20. Constructing a bipartite graph from a resistor network. The unlabeled internal edges on the right have weight 1.

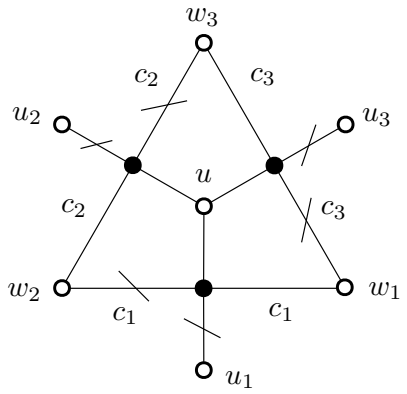

FIGURE 21. A small part of a vector-relation configuration coming from a resistor network.

Proof. The graph in Figure 21 shows a small piece of Γ. Consider each edge to have a negative sign if there is a stroke drawn through it and a positive sign otherwise. This picture can be tiled to cover the plane and define signs on all edges of Γ. The result satisfies the Kasteleyn condition: all faces are quadrilateral and each has either one or three negative edges on its boundary. As such, the edge weights coming from G multiplied by these signs give the relations of our vector-relation configuration.

The relations at the three black vertices in Figure 21 can now be read off as

$$\begin{aligned} u + c_1 w_1 - u_1 - c_1 w_2 &= 0 \\ u + c_2 w_2 - u_2 - c_2 w_3 &= 0 \\ u + c_3 w_3 - u_3 - c_3 w_1 &= 0 \end{aligned} \tag{6.1}$$

Dividing relation i by c_i and summing we obtain

$$\left(\frac{1}{c_1} + \frac{1}{c_2} + \frac{1}{c_3}\right) u - \frac{1}{c_1} u_1 - \frac{1}{c_2} u_2 - \frac{1}{c_3} u_3 = 0.$$

Therefore the projectivizations of u, u_1, u_2, u_3 all lie in a plane. These four points are precisely $Q_{i,j,k}$, $Q_{i+1,j+1,k}$, $Q_{i+1,j,k+1}$, $Q_{i,j+1,k+1}$ for some i, j, k. The relationship between the dynamics of resistor networks and the dimer model [13] guarantees that this property is preserved under the sequence of moves described in Section 3.2. The equivalence of the coplanarity condition to other definitions of Koenigs nets is given in [3, Theorem 2.29]. □

Remark 6.2. The relations of (6.1) can be rearranged to be instances of the discrete Moutard equation on the vectors at the white vertices. This description gives another path via [3, Theorem 2.32] to conclude that the Q-net is a discrete Koenigs net.

Remark 6.3. Let $G = (V, E)$ be a resistor network with weight function c. A *discrete harmonic function* is a function f on V, say with values in a vector space, satisfying the condition

$$\sum_{v'} c(\overline{vv'})(f(v) - f(v')) = 0$$

for all $v \in V$. The harmonic condition is equivalent to the existence of a second function g on V^* satisfying

$$g(w) - g(w') = c(\overline{vv'})(f(v) - f(v'))$$

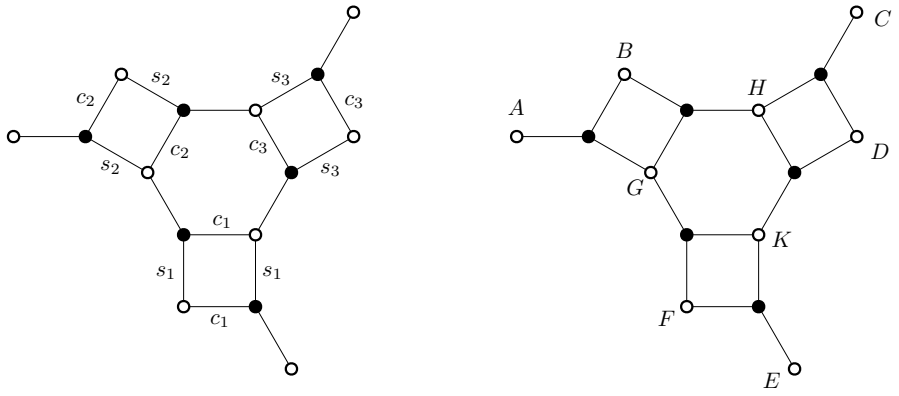

FIGURE 22. A bipartite graph coming from the Ising model.

for each dual edge pair $\overline{vv'} \in E$, $\overline{ww'} \in E^*$ (a convention needs to be fixed for the direction of the crossing of the edges). If G is the hexagonal grid, so G^* is the dual triangular grid, the above precisely means that f and g together define valid vectors for the associated vector-relation configuration on G. The picture is as in Figure 21 except with the non-trivial weights c_i moved to the other half of the edges. Some care with signs would be needed to extend this idea to other graphs.

We next consider the Ising model. We follow the approach of Galashin and Pylyavskyy [8]. Figure 22 gives an example of a bipartite graph arising from an Ising network. Each unlabeled edge has weight 1 and the s_i, c_i are certain positive reals satisfying $c_i^2 + s_i^2 = 1$. Roughly, the construction replaces each edge of the original graph with a copy of the $Gr_{2,4}$ plabic graph of Figure 18. In the case of Figure 22, the original graph consisted of a single triangle whose ith edge passes through both new edges marked s_i.

Proposition 6.4. *Consider a circuit configuration in $\mathbb{R}^3$ of the graph in Figure 22 with $A, B, \ldots \in \mathbb{P}^2$ the projectivizations of the points as indicated. Then the six points A, B, C, D, E, F lie on a conic.*

Proof. Let Y be the face weight of the hexagonal face and let Y_i for $i = 1, 2, 3$ be the weights of the quadrilateral faces. On the one hand, these can be computed in terms of the edge weights

$$Y = c_1c_2c_3$$
$$Y_i = \frac{s_i^2}{c_i^2} = \frac{1}{c_i^2} - 1$$

from which we get

$$Y^2(1+Y_1)(1+Y_2)(1+Y_3) = 1.$$

Meanwhile, by Proposition 2.6

$$Y = [G, B, H, D, K, F]^{-1}$$
$$Y_1 = -[F, G, K, E]^{-1} \qquad 1 + Y_1 = [F, K, E, G]$$
$$Y_2 = -[G, A, B, H]^{-1} \qquad 1 + Y_2 = [G, B, H, A]$$
$$Y_3 = -[H, C, D, K]^{-1} \qquad 1 + Y_3 = [H, D, K, C]$$

so

$$[G, B, H, D, K, F]^2 = [F, K, E, G][G, B, H, A][H, D, K, C].$$

Every factor occurring in $[G, B, H, D, K, F]$ appears once in the right hand side, and when canceled out, what remains is a triple ratio $[G, E, K, C, H, A]$. Therefore

$$[G, B, H, D, K, F] = [G, E, K, C, H, A].$$

The relative position of the points is as in the top left of Figure 14 and it follows from Carnot's Theorem that A, B, C, D, E, F lie on a conic. □

Now suppose we begin with an infinite triangular grid. The associated bipartite graph is the one in Figure 13 whose configurations correspond to discrete Darboux maps. What we have shown is that, in the notation of Definition 3.13, a Darboux map arising from the Ising model has the property that for all i, j, k the points

$$f^y_{i+1,j,k}, f^z_{i+1,j,k}, f^x_{i,j+1,k}, f^z_{i,j+1,k}, f^x_{i,j,k+1}, f^y_{i,j,k+1}$$

lie on a conic. This reduction of Darboux maps has been studied by Schief under the name *discrete CKP maps* [27].

Proposition 6.5. *Any discrete Darboux map arising from the Ising model on an infinite triangular grid is in fact a discrete CKP map.*

References

[1] Niklas Affolter. Miquel dynamics, Clifford lattices and the dimer model. arXiv:1808.04227.
[2] Niklas Affolter, Lie Fu, Max Glick, and Sanjay Ramassamy. *In progress.*
[3] Alexander I. Bobenko and Yuri B. Suris. *Discrete differential geometry*, volume 98 of *Graduate Studies in Mathematics*. American Mathematical Society, Providence, RI, 2008. Integrable structure.
[4] Adam Doliwa. Geometric discretisation of the Toda system. *Phys. Lett. A*, 234(3):187–192, 1997.
[5] Adam Doliwa and Paolo Maria Santini. Multidimensional quadrilateral lattices are integrable. *Phys. Lett. A*, 233(4-6):365–372, 1997.
[6] Julien Dubédat. Exact bosonization of the Ising model. arXiv:1112.4399.
[7] Vladimir Fock. Inverse spectral problem for GK integrable system. arXiv:1503.00289.
[8] Pavel Galashin and Pavlo Pylyavskyy. Ising model and the positive orthogonal Grassmannian. arXiv:1807.03282.
[9] Michael Gekhtman, Michael Shapiro, Serge Tabachnikov, and Alek Vainshtein. Higher pentagram maps, weighted directed networks, and cluster dynamics. *Electron. Res. Announc. Math. Sci.*, 19:1–17, 2012.
[10] Michael Gekhtman, Michael Shapiro, Serge Tabachnikov, and Alek Vainshtein. Integrable cluster dynamics of directed networks and pentagram maps. *Adv. Math.*, 300:390–450, 2016.
[11] Max Glick. The pentagram map and Y-patterns. *Adv. Math.*, 227(2):1019–1045, 2011.
[12] Max Glick and Pavlo Pylyavskyy. Y-meshes and generalized pentagram maps. *Proc. Lond. Math. Soc. (3)*, 112(4):753–797, 2016.
[13] Alexander B. Goncharov and Richard Kenyon. Dimers and cluster integrable systems. *Ann. Sci. Éc. Norm. Supér. (4)*, 46(5):747–813, 2013.
[14] Richard Kenyon. Lectures on dimers. arXiv:0910.3129.
[15] Richard Kenyon, Wai Yeung Lam, Sanjay Ramassamy, and Marianna Russkikh. Dimers and circle patterns. arXiv:1810.05616.
[16] Richard Kenyon and Andrei Okounkov. Planar dimers and Harnack curves. *Duke Math. J.*, 131(3):499–524, 2006.
[17] Richard Kenyon and Robin Pemantle. Double-dimers, the Ising model and the hexahedron recurrence. *J. Combin. Theory Ser. A*, 137:27–63, 2016.
[18] Richard W. Kenyon and Scott Sheffield. Dimers, tilings and trees. *J. Combin. Theory Ser. B*, 92(2):295–317, 2004.
[19] Allen Knutson, Thomas Lam, and David E. Speyer. Positroid varieties: juggling and geometry. *Compos. Math.*, 149(10):1710–1752, 2013.
[20] B. G. Konopelchenko and W. K. Schief. Menelaus' theorem, Clifford configurations and inversive geometry of the Schwarzian KP hierarchy. *J. Phys. A*, 35(29):6125–6144, 2002.
[21] Thomas Lam. Totally nonnegative Grassmannian and Grassmann polytopes. In *Current developments in mathematics 2014*, pages 51–152. Int. Press, Somerville, MA, 2016.
[22] Bernt Lindström. On the vector representations of induced matroids. *Bull. London Math. Soc.*, 5:85–90, 1973.
[23] Greg Muller and David E. Speyer. The twist for positroid varieties. *Proc. Lond. Math. Soc. (3)*, 115(5):1014–1071, 2017.
[24] Valentin Ovsienko, Richard Schwartz, and Serge Tabachnikov. The pentagram map: a discrete integrable system. *Comm. Math. Phys.*, 299(2):409–446, 2010.
[25] Alexander Postnikov. Positive grassmannian and polyhedral subdivisions. arXiv:1806.05307.
[26] Alexander Postnikov. Total positivity, Grassmannians, and networks. arXiv:0609764.
[27] Wolfgang Karl Schief. Lattice geometry of the discrete Darboux, KP, BKP and CKP equations. Menelaus' and Carnot's theorems. *J. Nonlinear Math. Phys.*, 10(suppl. 2):194–208, 2003.
[28] Richard Schwartz. The pentagram map. *Experiment. Math.*, 1(1):71–81, 1992.
[29] David Speyer. Variations on a theme of Kasteleyn, with application to the totally nonnegative Grassmannian. arXiv:1510.03501.
[30] Kelli Talaska. Combinatorial formulas for Γ-coordinates in a totally nonnegative Grassmannian. *J. Combin. Theory Ser. A*, 118(1):58–66, 2011.

Technische Universität Berlin, Institute of Mathematics, Strasse des 17. Juni 136, 10623 Berlin, Germany

Department of Mathematics, The Ohio State University, Columbus, OH 43210, USA

Department of Mathematics, University of Minnesota, Minneapolis, MN 55455, USA

Département de mathématiques et applications, École normale supérieure, CNRS, PSL University, 75005 Paris, France